

000 001 002 003 004 005 DEEP SPI: SAFE POLICY IMPROVEMENT VIA WORLD 006 MODELS 007 008 009

010 **Anonymous authors**
011 Paper under double-blind review
012
013
014
015
016
017
018
019
020
021
022
023
024

ABSTRACT

025 Safe policy improvement (SPI) offers theoretical control over policy updates,
026 yet existing guarantees largely concern offline, tabular reinforcement learning
027 (RL). We study SPI in general online settings, when combined with world model
028 and representation learning. We develop a theoretical framework showing that
029 restricting policy updates to a well-defined neighborhood of the current policy
030 ensures monotonic improvement and convergence. This analysis links transition
031 and reward prediction losses to representation quality, yielding online, “deep”
032 analogues of classical SPI theorems from the offline RL literature. Building on
033 these results, we introduce DeepSPI, a principled on-policy algorithm that couples
034 local transition and reward losses with regularised policy updates. On the ALE-57
035 benchmark, DeepSPI matches or exceeds strong behaviorals, including PPO and
036 DeepMDPs, while retaining theoretical guarantees.
037
038

1 INTRODUCTION

039 *Reinforcement learning* (RL) trains agents to act in complex environments through trial and error
040 (Sutton and Barto, 2018). To scale to high-dimensional domains, modern approaches rely on
041 function approximation, making *representation learning* (Echchahed and Castro, 2025) essential for
042 constructing latent spaces where behaviorally similar states are mapped close together and policies
043 and value functions become easier to estimate. A complementary approach is *model learning*, where
044 a predictive model of the environment is trained (Ha and Schmidhuber, 2018). Such models can be
045 leveraged for planning, generating simulated experience, or improving value estimates (Hafner et al.,
046 2021; Schrittwieser et al., 2020; Xiao et al., 2019).
047

048 In the online setting, where the agent updates its policy during interaction, avoiding catastrophic
049 errors is critical. Two key challenges arise: *out-of-trajectory (OOT) world models* and *confounding*
050 *policy updates*. OOT issues arise when the world model fails to capture rarely visited regions of
051 the state space, leading to unreliable predictions and unsafe updates when the latent policy explores
052 these regions (Suau et al., 2024). Confounding updates occur when both the policy and its underlying
053 representation are updated simultaneously: poor representations can lock the agent into suboptimal
054 behavior, while the policy itself prevents corrective updates to the representation. *Safe Policy*
055 *Improvement* (SPI) mitigates such risks by ensuring that new policies are not substantially worse than
056 their predecessors (Thomas et al., 2015). Classical SPI methods provide rigorous results in tabular
057 MDPs but depend on exhaustive state–action coverage, making them unsuitable for continuous or
058 high-dimensional spaces.
059

060 We address this gap by directly connecting representation and model learning with safe policy
061 improvement in complex environments with general state spaces. Our contributions are threefold.
062 First, we introduce a novel neighborhood operator that constrains policy updates, enabling policy
063 improvement with convergence guarantees. Second, we combine this operator with principled
064 model losses to bound the gap between a policy’s performance in the world model and in the true
065 environment, thereby enabling safe policy improvement in complex MDPs. This analysis also shows
066 that our scheme enforces representation quality by ensuring that states with similar values remain
067 close in the learned latent space. Third, we connect our theory to PPO (Schulman et al., 2017) and
068 propose DeepSPI, a practical algorithm that achieves strong empirical performance on the Arcade
069 Learning Environment (ALE; Bellemare et al. 2013) while retaining theoretical guarantees.
070
071

054 1.1 RELATED WORK
055

056 **Regularizing policy improvements.** Regularized updates, as in TRPO, PPO, and related analyses,
057 are now standard for stabilizing policy optimization (Schulman et al., 2015; 2017; Geist et al., 2019;
058 Kuba et al., 2022). Our work extends this perspective to the joint training of a world model and a
059 representation, where we constrain policy updates in a principled neighborhood while controlling
060 model quality through transition and reward losses.

061 **SPI** methods provide principled guarantees on policy updates from fixed datasets (offline RL)
062 (Thomas et al., 2015; Ghavamzadeh et al., 2016a; Laroche et al., 2019; Simão et al., 2020; Castellini
063 et al., 2023). These methods assume tabular state spaces and offline data, where error bounds must
064 hold globally across all state–action pairs, often via robust MDP formulations (Iyengar, 2005; Nilim
065 and Ghaoui, 2005). Our setting is fundamentally different: we study *online* RL with high-dimensional
066 inputs, where such global constraints are intractable. We take inspiration from the SPI literature but
067 introduce local, on-policy losses that make safe improvement feasible in practice. In spirit, other
068 model-based methods share the goal of providing SPI-like guarantees in more general settings, but
069 are again purely offline, omit any form of representation learning, and rely on assumptions that differ
070 substantially from ours (Yu et al., 2020; 2021; Kidambi et al., 2020).

071 **Representation learning and model-based RL.** Auxiliary transition and reward prediction losses
072 are central to many model-based methods, from DeepMDP to Dreamer and related world-model
073 approaches (Gelada et al., 2019; Hafner et al., 2021). In particular, the losses we consider for
074 learning transitions and rewards generalize a wide range of objectives used across the model-based
075 RL literature (François-Lavet et al., 2019; van der Pol et al., 2020; Kidambi et al., 2020; Delgrange
076 et al., 2022; Dong et al., 2023; Alegre et al., 2023). Conceptually, our representation guarantees are
077 related to the notions of state abstraction in MDPs (Li et al., 2006) and *bisimulation* (Larsen and Skou,
078 1991; Desharnais et al., 1998; Givan et al., 2003; Ferns et al., 2011). Building upon *bisimulation*,
079 works design representations that cluster states into groups where the agent is guaranteed to behave
080 similarly under the current policy (Castro, 2020; Zhang et al., 2021; Castro et al., 2021; Agarwal
081 et al., 2021a; Avalos et al., 2024). By contrast, we directly link representation quality and model
082 accuracy to our safe policy improvement analysis, yielding tractable guarantees in the online setting.

083 2 BACKGROUND
084

085 In the following, given a measurable space \mathcal{X} , we write $\Delta(\mathcal{X})$ for the set of distributions over \mathcal{X} . For
086 any distribution $\mu \in \Delta(\mathcal{X})$, we denote by $\text{supp}(\mu)$ its support.

088 **Markov Decision Processes** (MDPs) offer a formalism for sequential decision-making under uncer-
089 tainty. Formally, an MDP is a tuple of the form $\mathcal{M} = \langle \mathcal{S}, \mathcal{A}, P, R, s_I, \gamma \rangle$ consisting of a set of states
090 \mathcal{S} , actions \mathcal{A} , a transition function $P : \mathcal{S} \times \mathcal{A} \rightarrow \Delta(\mathcal{S})$, a bounded reward function $R : \mathcal{S} \times \mathcal{A} \rightarrow \mathbb{R}$
091 with $\|R\|_\infty = R_{\text{MAX}}$, an initial state $s_I \in \mathcal{S}$, and a discount factor $\gamma \in [0, 1]$. Unless otherwise stated,
092 we generally assume that \mathcal{S} and \mathcal{A} are compact. An agent interacting in \mathcal{M} produces *trajectories*, i.e.,
093 infinite sequences of states and actions $(s_t, a_t)_{t \geq 0}$ visited along the interaction so that $s_0 = s_I$ and
094 $s_{t+1} \sim P(\cdot | s_t, a_t)$ for all $t \geq 0$.

095 At each time step t , the agent selects an action according to a (stationary) *policy* $\pi : \mathcal{S} \rightarrow \Delta(\mathcal{A})$
096 mapping states to distributions over actions. Running an MDP under π induces a unique probability
097 measure \mathbb{P}_π over trajectories (Revuz, 1984), with associated expectation operator \mathbb{E}_π ; we write
098 $\mathbb{E}_\pi[\cdot | s_0 = s]$ when the initial state is fixed to $s \in \mathcal{S}$. A policy has *full support* if $\text{supp}(\pi(\cdot | s)) = \mathcal{A}$
099 for all $s \in \mathcal{S}$, and we denote the set of all policies by Π . A *stationary measure* of π is a distribution
100 over states visited under π , and is defined as a solution of $\xi_\pi(\cdot) = \mathbb{E}_{s \sim \xi_\pi} \mathbb{E}_{a \sim \pi(\cdot | s)} [P(\cdot | s, a)]$. Such
101 a measure is often assumed to exist in continual RL (Sutton and Barto, 2018), is *unique* in episodic
102 RL (Huang, 2020), and defines the *occupancy measure* in discounted RL (Metelli et al., 2023).¹

103 **Value functions.** The performance of the agent executing a policy $\pi \in \Pi$ in each single state
104 $s \in \mathcal{S}$ can be evaluated through the *value function* $V^\pi(s) = \mathbb{E}_\pi [\sum_{t=0}^{\infty} \gamma^t R(s_t, a_t) | s_0 = s]$. The
105 goal of an agent is to maximize the *return* from the initial state, given by $\rho(\pi, \mathcal{M}) = V^\pi(s_I)$.
106 To evaluate the quality of any action $a \in \mathcal{A}$, we consider the *action value function* $Q^\pi(s, a) =$

1¹Details on the formalization of episodic processes and value functions can be found in Appendix A.

108 $R(s, a) + \gamma \mathbb{E}_{s' \sim P(\cdot | s, a)} V^\pi(s')$, being the unique solution of Bellman’s equation with $V^\pi(s) =$
 109 $\mathbb{E}_{a \sim \pi(\cdot | s)} Q^\pi(s, a)$. Alternatively, any given action can be evaluated through the *advantage function*
 110 $A^\pi(s, a) = Q^\pi(s, a) - V^\pi(s)$, giving the advantage of selecting an action over the current policy.
 111

112 **Representation learning in RL.** In realistic environments, the state–action space is too large for
 113 tabular policies or value functions. Instead, deep RL employs an encoder $\phi: \mathcal{S} \rightarrow \bar{\mathcal{S}}$ that maps states
 114 to a tractable *latent space* $\bar{\mathcal{S}}$, from which value functions can be approximated. Learning such encoders
 115 is referred to as *representation learning* (Echchahed and Castro, 2025). To improve representations,
 116 agents are often trained with additional objectives, commonly *auxiliary tasks* requiring predictive
 117 signals. Policy-based methods then optimize a *latent policy* $\bar{\pi}: \bar{\mathcal{S}} \rightarrow \Delta(\mathcal{A})$ jointly with ϕ , executed
 118 in the environment as $\bar{\pi}(\cdot | \phi(s))$. By convention, we write $\bar{\pi}(\cdot | s)$ for $\bar{\pi} \circ \phi(s)$ when ϕ is clear, and
 119 denote the set of all latent policies by $\bar{\Pi}$. For any $\bar{\pi} \in \bar{\Pi}$, the composed policy $\bar{\pi} \circ \phi$ belongs to Π .
 120

121 **Model-based RL** augments policy learning with a *world model* $\bar{\mathcal{M}} = \langle \bar{\mathcal{S}}, \mathcal{A}, \bar{P}, \bar{R}, \bar{s}_I, \gamma \rangle$, which can
 122 improve (i) sample efficiency by generating trajectories (e.g., Hafner et al. 2021), (ii) value estimation
 123 through planning (e.g., Buckman et al. 2018), and (iii) representation learning by grouping states
 124 with similar behavior (e.g., Gelada et al. 2019; Zhang et al. 2021). When $\bar{\mathcal{S}} = \mathcal{S}$, the model must
 125 replicate environment dynamics, which is often intractable. Instead, we focus on $\bar{\mathcal{S}}$ defined by the
 126 learned representation ϕ , so that $\bar{\mathcal{M}}$ becomes an abstraction of \mathcal{M} . Learning transition and reward
 127 functions then additionally serves as an auxiliary signal for the representation, encouraging states
 128 with similar behavior to map close in $\bar{\mathcal{S}}$. Since $\bar{\mathcal{S}}$ is the latent space, $\bar{\Pi}$ corresponds to the policies of
 129 $\bar{\mathcal{M}}$. We further assume $\bar{\mathcal{S}}$ is equipped with a metric $\bar{d}: \bar{\mathcal{S}} \times \bar{\mathcal{S}} \rightarrow [0, \infty)$ to measure distances.
 130

3 NO WAY HOME: WHEN WORLD MODELS AND POLICIES GO OUT OF TRAJECTORIES

133 World models are usually learned toward minimizing a **reward loss** L_R and/or **transition loss** L_P
 134 from experiences η collected along the agent’s trajectories. Those experiences are either gathered
 135 in the form of a *batch* or a *replay buffer* \mathcal{B} . In general, the loss functions take the following form:
 136 $L_R = \mathbb{E}_{\eta \sim \mathcal{B}} f_R(\phi, \bar{R}; \eta)$ and $L_P = \mathbb{E}_{\eta \sim \mathcal{B}} f_P(\phi, \bar{P}; \eta)$, where f_R (resp. f_P) assign a “cost” relative
 137 to the error between R and \bar{R} (resp. P and \bar{P}) according to the experiences η and their representation.
 138 Henceforth, we refer to the policy π_b used to insert experiences in \mathcal{B} as the **behavioral policy**.
 139

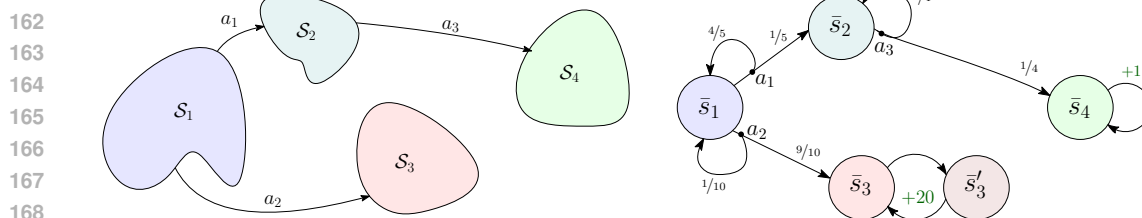
3.1 OUT-OF-TRAJECTORY WORLD MODEL

140 One may consider leveraging the model $\bar{\mathcal{M}}$ to improve the policy π_b . This can be achieved by
 141 directly planning a new policy $\bar{\pi}$ in $\bar{\mathcal{M}}$ or drawing imagined trajectories in the world model to
 142 evaluate new actions and improve on sample complexity during RL. However, since the world model
 143 is learned from experiences stored in \mathcal{B} , we can only be certain of its average accuracy according
 144 to this data. This is problematic because some regions of the state space of \mathcal{M} may have been
 145 rarely, or not at all, visited under π_b . In that case, the predictions made in $\bar{\mathcal{M}}$ might cause the agent
 146 to “hallucinate” inaccurate trajectories in the latent space and spoil the policy improvement. This
 147 problem, known as the **out-of-trajectory** (OOT) issue (Suau et al., 2024), arises when a policy in $\bar{\mathcal{M}}$
 148 deviates substantially from π_b , which can render the model unreliable.
 149

150 To illustrate this problem, consider the world model of Figure 1. Assume the model is trained by
 151 collecting trajectories produced by π_b in \mathcal{M} where $\pi_b(a_2 | s) \leq \epsilon$ for all $s \in \mathcal{S}_1$, with $\epsilon > 0$. For
 152 a sufficiently small ϵ , the region \mathcal{S}_3 in the original environment would remain largely unexplored
 153 while having almost no impact on the losses L_R, L_P . Therefore, the representation of states in \mathcal{S}_3
 154 (\bar{s}_3 and \bar{s}'_3) may turn completely inaccurate. Here, the model incorrectly assigns a reward of 20 to \bar{s}'_3 ,
 155 whereas the true reward is strictly negative. Consequently, the optimal policy in $\bar{\mathcal{M}}$ deterministically
 156 selects a_2 in \bar{s}_1 . When executed in the original environment, this policy drives the agent to \mathcal{S}_3 thereby
 157 degrading the behavioral policy π_b .
 158

3.2 CONFOUNDING POLICY UPDATE

159 Updating both the representation and the policy solely from experience collected under a behavioral
 160 policy can *degrade* performance rather than improve it. In the same spirit as *policy confounding*
 161 (Suau et al., 2024), we call this phenomenon **confounding policy update**. The MDP in Figure 2
 162 illustrates the issue.
 163



162
163
164
165
166
167
168
169
170
(a) A large MDP \mathcal{M} whose state space is divided in four
regions $\mathcal{S} = \bigcup_{i=1}^4 \mathcal{S}_i$.

171
172
173
174
175
176
177
178
179
180
181
182
183
184
185
186
187
188
189
190
191
192
193
194
195
196
197
198
199
200
201
202
203
204
205
206
207
208
209
210
211
212
213
214
215
(b) A simple world model $\bar{\mathcal{M}}$ whose state space is
 $\bar{\mathcal{S}} = \{\bar{s}_1, \bar{s}_2, \bar{s}_3, \bar{s}_3', \bar{s}_4\}$.

Figure 1: In \mathcal{M} , continuously playing a_1 in states from \mathcal{S}_1 eventually leads the agent to the region \mathcal{S}_2 , and playing a_3 in \mathcal{S}_2 eventually leads the agent to \mathcal{S}_4 where a reward of 1 is incurred at each time step, whatever the action played. Playing a_2 in \mathcal{S}_1 leads the agent to the region \mathcal{S}_3 , where all actions incur negative rewards. Here, $\phi(s) = \bar{s}_i$ for any $s \in \mathcal{S}_i$ and $i = \{1, 2, 4\}$. For $s \in \mathcal{S}_3$, we have either $\phi(s) = \bar{s}_3$ or $\phi(s) = \bar{s}_3'$.

The agent maps the states s_2 and s_3 to the *same* latent state \bar{s} , i.e. $\phi(s) = \bar{s}$ iff $s \in \{s_2, s_3\}$. States s_1 and s_4 each have their own latent state. We consider the behavioral policy $\pi_b := \bar{\pi}_b \circ \phi$, where $\bar{\pi}_b$ is a stochastic policy with a small exploration rate ζ :

$$\bar{\pi}_b(a_1 \mid \bar{s}) = 1 - \zeta, \quad \bar{\pi}_b(a_2 \mid \bar{s}) = \zeta, \quad (1)$$

for $0 < \zeta \ll \epsilon$. A good representation would ideally group states from which the agent behaves similarly. Because trajectories that reach s_3 and pick a_2 are unlikely, the two states appear identical under π_b : $|V^{\pi_b}(s_2) - V^{\pi_b}(s_3)| \approx 0$. Therefore, this justifies using ϕ as representation for π_b , because the values of s_2 and s_3 are nearly identical: the agent exhibits close behaviors under π_b from those states.

Suppose exploration under $\bar{\pi}_b$ eventually discovers that playing a_2 in \bar{s} sometimes yields the +2 reward. Based on exploration data, an RL agent might therefore be tempted to change the latent policy to $\bar{\pi}(a_2 \mid \bar{s}) = 1$ without modifying the representation ϕ . With the representation still grouping s_2 and s_3 , the new policy would now deterministically pick a_2 in *both* concrete states. Whenever the agent actually reaches s_3 , it would receive the large negative reward $-2/\epsilon$, which turns the overall return (from s_1) negative, thus *worse* than under π_b even though a_2 is indeed optimal in s_2 .

A solution to this problem would have been to split the representation of s_2 and s_3 in two distinct latent states. In general, representation and policy learning must be *coupled* since any change in the policy that alters the distribution over states can invalidate a previously adequate representation. However, in this example, the agent has no incentive to do so based on the experiences collected under π_b . As we will show below, updating both the policy and the representation jointly should be handled carefully to ensure *policy improvement*.

Our goal is to *establish sufficient conditions* to guarantee **safe policy improvement** during the RL process, either based on world models, state representations, or both, thus alleviating OOT world model and confounding policy update issues. Notice that, in the examples, both problems occur when performing *aggressive* updates from π_b to a new policy $\bar{\pi}$ (the mode of the distributions drastically shifts). Intuitively, *smooth* updates indeed ensure to alleviate those issues: constraining the policy search to policies “close” to π_b (i) prevents hallucinations in parts of the world model that have been underexplored; (ii) reduces the risk of significantly degrading the return when updating the policy. While the benefits of regularizing policy improvements have already been both theoretically and practically justified (e.g., Geist et al. 2019; Kuba et al. 2022), their implications when mixing model-based and representation learning in RL have been underexplored.

Roadmap. To rigorously address the OOT and confounding-update issues, the next sections develop the theoretical foundations of our approach, showing how controlled policy updates, local model losses, and representation stability interact. We briefly summarize how the main results connect.

Our analysis combines **neighborhood-restricted policy updates**, **model-quality bounds**, and **representation guarantees**. Sect. 4 introduces the neighborhood operator defining a trust region around the behavioral policy; restricting updates to this region ensures monotonic improvement and convergence (Thm. 1). Sect. 5 then links the reward and transition losses to value discrepancies:

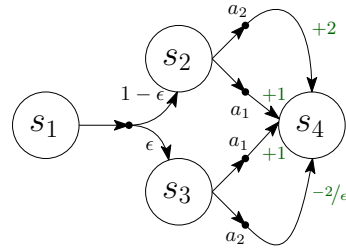


Figure 2: MDP where the probability of transitioning from s_1 to s_2 is $1 - \epsilon$, for $0 < \epsilon < 1/4$.

216 Thm. 2 shows that, when these losses are small, and updates remain in the neighborhood, the world
 217 model stays accurate under the learned representation. Combining these ingredients yields our
 218 first SPI result (Thm. 3), guaranteeing that direct policy updates in the world model translate to
 219 improvement under controlled error. Finally, Thm. 4 shows that the same loss-based control stabilizes
 220 the encoder, ensuring that value-distinct states remain separated in the latent space.
 221

222 4 YOUR FRIENDLY NEIGHBORHOOD POLICY

224 Motivated by the intuition that constraining policy updates can mitigate OOT and confounding policy
 225 issues, we consider measuring the update as the **importance ratio** (IR) of the policies. This measure
 226 provides guarantees for constraining policy and representation updates, and with an appropriate
 227 optimisation scheme, ensures both policy improvement and convergence. In Section 5, we will further
 228 show that properly constraining the IR allows for safe policy improvements in world models while
 229 providing representation guarantees.

230 Let $\pi, \pi' \in \Pi$, the **extremal importance ratios** are defined as $D_{\text{IR}}^{\text{ext}}(\pi, \pi') =$
 231 $\text{ext}\{\pi'(a|s)/\pi(a|s) : s \in \mathcal{S}, a \in \text{supp}(\pi(\cdot|s))\}$, where $\text{ext} \in \{\inf, \sup\}$. We define a **neighbor-**
 232 **hood operator**² based on the IR, $\mathcal{N}^C : \Pi \rightarrow 2^\Pi$ for some constant $1 < C < 2$, establishing a
 233 trust region for policies updates that constraints the IR between $2 - C$ and C :

$$235 \mathcal{N}^C(\pi) = \left\{ \pi' \in \Pi \mid \begin{array}{l} 2 - C \leq D_{\text{IR}}^{\text{inf}}(\pi, \pi') \leq D_{\text{IR}}^{\text{sup}}(\pi, \pi') \leq C, \\ \text{and } \text{supp}(\pi(\cdot|s)) = \text{supp}(\pi'(\cdot|s)) \quad \forall s \in \mathcal{S} \end{array} \right\} \quad \forall \pi \in \Pi. \quad (2)$$

238 A critical question is whether an agent that restricts its policy updates to a defined neighborhood is
 239 truly following a sound **policy improvement** scheme. The following theorem shows that it does and
 240 further guarantees convergence.

241 **Theorem 1.** (Policy improvement and convergence guarantees) Assume \mathcal{S} and \mathcal{A} are finite spaces.
 242 Let $\pi_0 \in \Pi$ be a policy with full support and $(\pi_n)_{n \geq 0}$ be a sequence of policy updates defined as

$$244 \pi_{n+1} := \arg \sup_{\pi' \in \mathcal{N}^C(\pi_n)} \mathbb{E}_{s \sim \mu_{\pi_n}} \mathbb{E}_{a \sim \pi'(\cdot|s)} A^{\pi_n}(s, a), \quad (3)$$

246 where μ_{π_n} is a sampling distribution with $\text{supp}(\mu_{\pi_n}) = \mathcal{S}$ for each $n \geq 0$. Then, the value function
 247 V^{π_n} is monotonically improving, converges to V^* , and so is the return $\rho(\pi_n, \mathcal{M})$.

248 The proof consists in showing the resulting policy update scheme is an instance of *mirror learning*
 249 (Kuba et al., 2022), which yields the guarantees. Notice that since π_0 has full support, all the
 250 subsequent policies π_n have full support as well. To maintain the guarantees, considering a stationary
 251 measure ξ_{π_n} as the sampling distribution is only possible when $\text{supp}(\xi_{\pi_n}) = \mathcal{S}$. Note that this is
 252 always the case in episodic tasks (as the policy itself has full support). This is more generally true in
 253 ergodic MDPs (Puterman, 1994).

255 5 WITH GREAT WORLD MODELS COMES GREAT REPRESENTATION

257 This section explains how the neighborhood operator of Eq. 2 enables safe policy improvement during
 258 world-model planning and representation updates in complex environments. Standard SPI methods
 259 ignore representation learning and require exhaustive state-action coverage in \mathcal{B} to obtain guarantees,
 260 making them unsuitable for general state-action spaces. Even in finite domains, bounding the count
 261 of each state-action pair does not scale. Laroche et al. (2019) proposed *baseline bootstrapping* for
 262 under-sampled pairs, but their approach remains impractical in large-scale settings despite conceptual
 263 similarities to our operator. Further discussion of SPI limitations is provided in Appendix D.

264 **Learning an accurate world model.** SPI typically relies on optimizing a policy with respect to
 265 a latent model learned from the data stored in \mathcal{B} . In contrast to previous methods, our approach
 266 scales to high-dimensional feature spaces by (i) learning a representation ϕ and (ii) considering **local**
 267 **error measures** as opposed to global measures across the whole state-action space. We formalize

269 ²There are clear similarities between the IR, our neighborhood operator, and the PPO loss function (Schulman
 et al., 2017). We discuss this connection in Section 6.

them as tractable *loss functions*. Their local nature makes them compliant with stochastic gradient descent methods. Formally, given a distribution $\mathcal{B} \in \Delta(\mathcal{S} \times \mathcal{A})$, we define the *reward loss* $L_R^{\mathcal{B}}$ and the *transition loss* $L_P^{\mathcal{B}}$ as

$$L_R^{\mathcal{B}} := \mathbb{E}_{s,a \sim \mathcal{B}} |R(s,a) - \bar{R}(\bar{s},a)|, \quad L_P^{\mathcal{B}} := \mathbb{E}_{s,a \sim \mathcal{B}} \mathcal{W}(\phi_{\sharp} P(\cdot | s,a), \bar{P}(\cdot | \phi(s),a)) \quad (4)$$

where $\phi_{\sharp} P$ is the *pushforward measure* of P by ϕ , and \mathcal{W} the *Wasserstein distance* (Vaserstein, 1969). \mathcal{W} between $\mu, \nu \in \Delta(\bar{\mathcal{S}})$ is defined as $\mathcal{W}(\mu, \nu) = \inf_{\lambda \in \Lambda(\mu, \nu)} \mathbb{E}_{(\bar{s}, \bar{s}') \sim \lambda} \bar{d}(\bar{s}, \bar{s}')$, where $\Lambda(\mu, \nu)$ is the set of all couplings of μ and ν . While the Wasserstein operator may seem scary at first glance, it generalizes over transition losses that can be found in the literature (cf. Sect. 1.1). In particular, when the latent space is discrete, this distance boils down to the *total variation distance*. Another notable case is when the transition dynamics are deterministic, in which case the transition loss reduces to $L_P^{\mathcal{B}} = \mathbb{E}_{s,a,s' \sim \mathcal{B}} \bar{d}(\phi(s'), \bar{P}(\phi(s),a))$. Finally, in general, a tractable upper bound can be obtained as $L_P^{\mathcal{B}} \leq \mathbb{E}_{s,a,s' \sim \mathcal{B}} \mathbb{E}_{\bar{s}' \sim \bar{P}(\cdot | \phi(s),a)} \bar{d}(\phi(s'), \bar{s}')$ (proof in Appendix C).

Lipschitz constants. To provide the guarantees, for any particular policy $\bar{\pi} \in \bar{\Pi}$, we assume the world model is equipped with *Lipschitz constants* $K_{\bar{R}}^{\bar{\pi}}, K_{\bar{P}}^{\bar{\pi}}$ defined as follows: for all $\bar{s}_1, \bar{s}_2 \in \bar{\mathcal{S}}$,

$$\begin{aligned} \left| \mathbb{E}_{a_1 \sim \bar{\pi}(\cdot | \bar{s}_1)} \bar{R}(\bar{s}_1, a_1) - \mathbb{E}_{a_2 \sim \bar{\pi}(\cdot | \bar{s}_2)} \bar{R}(\bar{s}_2, a_2) \right| &\leq K_{\bar{R}}^{\bar{\pi}} \cdot \bar{d}(\bar{s}_1, \bar{s}_2), \\ \mathcal{W} \left(\mathbb{E}_{a_1 \sim \bar{\pi}(\cdot | \bar{s}_1)} \bar{P}(\cdot | \bar{s}_1, a_1), \mathbb{E}_{a_2 \sim \bar{\pi}(\cdot | \bar{s}_2)} \bar{P}(\cdot | \bar{s}_2, a_2) \right) &\leq K_{\bar{P}}^{\bar{\pi}} \cdot \bar{d}(\bar{s}_1, \bar{s}_2). \end{aligned}$$

Intuitively, the Lipschitzness of the latent reward and transition functions guarantees that the latent space is well-structured, so that nearby latent states exhibit similar latent dynamics. Gelada et al. (2019) control those bounds by adding a *gradient penalty term* to the loss and enforce Lipschitzness (Gulrajani et al., 2017). One can also obtain constrained Lipschitz constants as a side effect by enforcing the metric \bar{d} to match the *bisimulation distance* in the latent space (Zhang et al., 2021). Interestingly, when the latent space is discrete, Lipschitz constants can be trivially inferred since $K_{\bar{R}}^{\bar{\pi}} = 2R_{\text{MAX}}$ and $K_{\bar{P}}^{\bar{\pi}} = 1$ (Delgrange et al., 2022). Note also that as the spaces are assumed compact, restricting to continuous functions ensures Lipschitz continuity.

For the sake of presentation, we restrict our attention to the following assumption for Thms. 2 and 3:

Assumption 1. *We assume that the agent operates in the episodic RL setting, i.e., we consider the standard RL framework where the environment is eventually reset with probability one.*

Our results extend to general settings where a stationary distribution is accessible (c.f. Remark 3).

World model quality. Before introducing our safe policy improvement theorem, we first show that the local losses effectively measure the world model’s quality with respect to the original environment. Namely, their difference in return obtained **under any latent policy in a well-defined neighborhood** is bounded by the local losses **derived from the reference, behavioral policy’s state-action distribution**. This is formalized in the following theorem.

Theorem 2. *Suppose $\gamma > 1/2$ and $K_{\bar{P}}^{\bar{\pi}} < 1/\gamma$. Let $C \in (1, 1/\gamma)$, $\pi_b \in \Pi$ be the base policy, $(\bar{\pi} \circ \phi) \in \mathcal{N}^C(\pi_b)$ where $\bar{\pi} \in \bar{\Pi}$ is a latent policy and $\phi: \mathcal{S} \rightarrow \bar{\mathcal{S}}$ a state representation. Then,*

$$|\rho(\bar{\pi} \circ \phi, \mathcal{M}) - \rho(\bar{\pi}, \bar{\mathcal{M}})| \leq \text{AEL}(\pi_b) \cdot \frac{L_R^{\xi_{\pi_b}}/\gamma + K_V \cdot L_P^{\xi_{\pi_b}}}{1/D_{IR}^{\text{sup}}(\pi_b, \bar{\pi}) - \gamma},$$

where $\text{AEL}(\pi_b)$ denotes the average episode length when \mathcal{M} runs under π_b , $K_V = K_{\bar{R}}^{\bar{\pi}}/(1 - \gamma K_{\bar{P}}^{\bar{\pi}})$, and $L_R^{\xi_{\pi_b}}, L_P^{\xi_{\pi_b}}$ are the local losses of Eq. 4 over the stationary distribution ξ_{π_b} induced by π_b .

In simpler terms, if the deviation (supremum IR, or SIR for short) between the behavioral policy and **any new policy** $\bar{\pi}$ stays strictly lower than $1/\gamma$, the gap in return between the environment and the world model for this new policy can be bounded using data collected via π_b . Minimizing local losses from π_b ’s data ensures that refining the representation ϕ for $\bar{\pi}$ improves model quality: when these losses vanish, \mathcal{M} and $\bar{\mathcal{M}}$ are almost surely equivalent under $\bar{\pi}$. The bound depends on the Average Episode Length (AEL), but even a loose upper bound is sufficient to preserve guarantees. It is also

324 strongly influenced by the discount factor γ , which defines an implicit horizon. Smaller values permit
 325 larger deviations from π_b and relax the accuracy required of the world model.
 326

327 **Safe policy improvement.** We consider the setting where the world model is used to improve the
 328 behavioral policy $\pi_b = \bar{\pi}_b \circ \phi$, with $\bar{\pi}_b \in \bar{\Pi}$ and the representation ϕ is fixed during each update.
 329 Restricting updates to a well-defined neighborhood guarantees that $\rho(\bar{\pi} \circ \phi, \mathcal{M}) - \rho(\pi_b, \mathcal{M}) \geq$
 330 $\rho(\bar{\pi}, \mathcal{M}) - \rho(\bar{\pi}_b, \mathcal{M}) - \zeta$, where ζ is defined as the cumulative *modeling error* from the local losses.

331 **Theorem 3.** (Deep, Safe Policy Improvement) *Under the same preamble as in Thm. 2, assume that ϕ
 332 is fixed during the policy update and the behavioral is a latent policy with $\pi_b := \bar{\pi}_b \circ \phi$ and $\bar{\pi}_b \in \bar{\Pi}$.
 333 Then, the improvement of the return of \mathcal{M} under $\bar{\pi}$ can be guaranteed on π_b as*

$$334 \quad \rho(\bar{\pi} \circ \phi, \mathcal{M}) - \rho(\pi_b, \mathcal{M}) \geq \rho(\bar{\pi}, \mathcal{M}) - \rho(\bar{\pi}_b, \mathcal{M}) - \zeta,$$

$$335 \quad \text{where } \zeta := \text{AEL}(\pi_b) \cdot \left(L_R^{\xi_{\pi_b}} / \gamma + K_V L_P^{\xi_{\pi_b}} \right) \left(\frac{1}{1/D_{IR}^{\text{sup}}(\pi_b, \bar{\pi})} + \frac{1}{1-\gamma} \right).$$

338 Theorem 3 addresses the OOT issue (Section 3.1): if the SIR of the behavioral remains strictly below
 339 $1/\gamma$, then minimizing the local losses reduces the error ζ , ensuring safe policy improvement when
 340 the world model is used to enhance the policy. While our focus is not on offline SPI, Appendix E
 341 (Thm. 5) additionally provides a PAC variant of the result, following the standard use of confidence
 342 bounds in the SPI literature.

343 **Representation learning.** Finally, we analyze how learning a world model using our loss functions
 344 as an auxiliary task facilitates the learning of a useful representation. A good representation should
 345 ensure that environment states that are close in the representation also have close values, directly
 346 supporting policy learning. Specifically, we seek “almost” Lipschitz continuity (Vanderbei, 1991) of
 347 the form $\exists K : \forall s_1, s_2 \in \mathcal{S}, |V^{\pi_b}(s_1) - V^{\pi_b}(s_2)| \leq K \cdot \bar{d}(\phi_{\text{old}}(s_1), \phi_{\text{old}}(s_2)) + \mathcal{L}_{\pi_b}(\phi_{\text{old}})$ where \mathcal{L}_{π_b}
 348 is an auxiliary loss **depending on the data collected by π_b .** Notably, a critical question is whether
 349 updating the policy and its representation, respectively to $\bar{\pi}$ and ϕ , maintains Lipschitz continuity.
 350 Crucially, as the behavioral π_b is updated to $\bar{\pi} \circ \phi$ with respect to the experience collected under
 351 π_b , the bound must hold for \mathcal{L}_{π_b} . The following theorem is a probabilistic version of this statement,
 352 formalized as a concentration inequality:

353 **Theorem 4.** (Deep SPI for representation learning) *Under the same preamble as in Thm. 2, let
 354 $\varepsilon > 0$ and $\delta := 4 \cdot \frac{L_R^{\xi_{\pi_b}} + \gamma K_V \cdot L_P^{\xi_{\pi_b}}}{\varepsilon \cdot (1/D_{IR}^{\text{sup}}(\pi_b, \bar{\pi}) - \gamma)}$. Then, with probability at least $1 - \delta$ under ξ_{π_b} , we have for all
 355 $s_1, s_2 \in \mathcal{S}$ that*

$$356 \quad |V^{\bar{\pi}}(s_1) - V^{\bar{\pi}}(s_2)| \leq K_V \cdot \bar{d}(\phi(s_1), \phi(s_2)) + \varepsilon.$$

358 Theorem 4 addresses confounding policy updates (Section 3.2): minimizing the losses increases the
 359 probability that learned representations remain almost Lipschitz under controlled policy changes (with
 360 an SIR below $1/\gamma$). This prevents distinct states from collapsing into identical latent representations
 361 that degrade performance. We note that Gelada et al. (2019) proved a similar bound when $\pi_b = \bar{\pi}$
 362 (the policy update was disregarded), which in contrast to ours, *surely* holds with

$$363 \quad \varepsilon := \frac{L_R^{\xi_{\bar{\pi}}} + \gamma K_V \cdot L_P^{\xi_{\bar{\pi}}}}{1-\gamma} \cdot \left(\frac{1}{\xi_{\bar{\pi}}(s_1)} + \frac{1}{\xi_{\bar{\pi}}(s_2)} \right).$$

366 However, in general spaces, for any specific $s \in \mathcal{S}$, $\xi_{\bar{\pi}}(s)$ might simply equal zero, making the bound
 367 undefined. In particular, in the continuous setting, \mathcal{S} is widely assumed to be endowed with a Borel
 368 sigma-algebra, where the probability of every single point is indeed zero.

370 6 ACROSS THE SPI-VERSE: PPO COMES INTO PLAY

372 These theorems inspire a practical RL algorithm that combines policy improvement and guarantees
 373 with solid empirical performance. The critical part of our approach is to make sure updates are
 374 restricted to the policy neighborhood while minimizing the auxiliary losses L_R, L_P . In fact, our
 375 neighborhood operator has close connections to PPO (Schulman et al., 2017), where the policy update
 376 is given by³

377 ³we give the formulation of Kuba et al. (2022), which is equal to the one of Schulman et al. (2017).

$$\pi_{n+1} := \arg \sup_{\pi' \in \Pi} \mathbb{E}_{s \sim \xi_{\pi_n}} \left[\mathbb{E}_{a \sim \pi'(\cdot|s)} A^{\pi_n}(s, a) - \mathfrak{D}_{\pi_n}(\pi' | s) \right], \quad (5)$$

with $\mathfrak{D}_{\pi_n}(\pi' | s) = \mathbb{E}_{a \sim \pi_n(\cdot|s)} \text{ReLU} \left([\pi'(a|s)/\pi_n(a|s) - \text{clip}(\pi'(a|s)/\pi_n(a|s), 1 \pm \epsilon)] \cdot A^{\pi_n}(s, a) \right)$, for some $\epsilon > 0$. By fixing $\epsilon = C - 1$, instead of strictly constraining the updates to the neighborhood, the regularization $\mathfrak{D}_{\pi_n}(\pi' | s)$ corrects the utility $\mathbb{E}_{a \sim \pi'(\cdot|s)} A^{\pi_n}(s, a)$ (compare Eq. 3 and Eq. 5), so that there is no incentive for π' to deviate from π_n with an IR outside the range $[2 - C, C]$. Under the same assumption as in Theorem 1, PPO is also an instance of mirror learning (Kuba et al., 2022), meaning it also benefits from the same convergence guarantees.

Strictly restricting the IR in a neighborhood is much harder in practice, considering a PPO objective is thus an appealing alternative. However, it is not sufficient to add the auxiliary losses L_P, L_R to the objective of Eq. 5 to maintain the guarantees. Indeed, updating the representation ϕ by minimizing the additional losses may push the the policy $\bar{\pi} \circ \phi$ outside the neighborhood. As a solution we propose to incorporate the local losses by replacing all occurrences of A^{π_n} in Eq. 5 by the utility

$$U^{\pi_n}(s, a, s') := A^{\pi_n}(s, a) - \alpha_R \cdot \ell_R(s, a) - \alpha_P \cdot \ell_P(s, a, s'), \quad (6)$$

where $\ell_R(s, a) := |R(s, a) - \bar{R}(\phi(s), a)|$, $\ell_P(s, a, s') := \mathbb{E}_{\bar{s}' \sim \bar{P}(\cdot|\phi(s), a)} \bar{d}(\phi(s'), \bar{s}')$, $s' \sim P(\cdot | s, a)$, and $\alpha_R, \alpha_P \in (0, 1]$. Intuitively, ℓ_R, ℓ_P are transition-wise auxiliary losses that allow retrieving $L_R^{\xi_{\pi_n}}$ and $L_P^{\xi_{\pi_n}}$ in expectation w.r.t. the current policy π_n . When optimized, since they are clipped in a PPO-fashion, U^{π_n} allows restricting the policy updates to the neighborhood.

Algorithm 1: DeepSPI

Inputs: Horizon T , batch size B , vectorized environment `env`, parameters θ
 Initialize vectors
 $s \in \mathcal{S}^{(T+1) \times B}, a \in \mathcal{A}^{T \times B}, r \in \mathbb{R}^{T \times B}$
repeat
for $t \leftarrow 1$ to T **do**
 Draw actions from the current policy:
 $a_{t,i} \sim \bar{\pi}(\cdot | \phi(s_{t,i})) \quad \forall 1 \leq i \leq B$
 Perform a single parallelized (B) step:
 $r_t, s_{t+1} \leftarrow \text{env.step}(s_t, a_t)$
 Update θ by descending
 $\nabla_{\theta} \text{DeepSPI_loss}(s, a, r, U^{\bar{\pi} \circ \phi}, \theta)$
 \triangleright change A in Eq. 5 by U from Eq. 6
 $s_1 \leftarrow s_{T+1}$
until convergence
return θ

6.1 ILLUSTRATIVE EXAMPLE

To illustrate the representation learning capabilities of DeepSPI, we consider the toy grid-world shown in Fig. 3. This environment mirrors the confounding policy update discussed in Sect. 3.2, instantiated earlier in Fig. 2.

The agent starts in the cell labeled I. Upon leaving the orange cell immediately to its right, it is sent to the top branch with probability $1 - \epsilon$ and to the bottom branch with probability ϵ . It must then traverse a corridor of n blue cells (here $n=5$). Moving one cell to the right yields a reward of $+1$, and the agent cannot move backwards.

At the final corridor cell, marked with a \star , moving right yields a reward of $+1$ regardless of whether the agent is in the top or bottom branch, and the episode terminates. *The difference is when the agent moves up from the \star cell:* in the top branch, it receives a reward of $+\gamma^n/\gamma^n$, whereas in the bottom branch it receives $-(2-\epsilon)\gamma^n/(\epsilon\gamma^n)$ before termination. As in Sect. 3.2, this construction ensures that if both \star states are merged in the latent space, choosing “right” remains acceptable (their values coincide), but choosing “up” produces a negative expected return from the initial state I (details in

From this loss, we propose DeepSPI, a **principled algorithm leveraging the policy improvement and representation learning capabilities developed in our theory**. As our losses rely on distributions defined over the current policy, we focus on the on-policy setting. While model-based approaches are not standard in this setting, we stress that **highly parallelized collection of data** (e.g., via vectorized environments) **enables a wide coverage of the state space** (cf. Mayor et al., 2025; Gallici et al., 2025), which is suitable to optimize the latent model. DeepSPI updates the world model, the encoder, and the policy simultaneously while guaranteeing the representation is suited to perform safe policy updates.

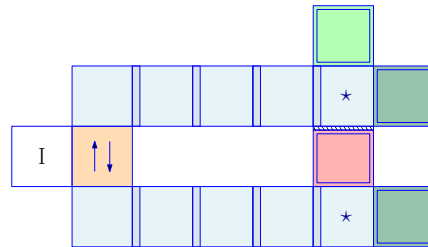


Figure 3: Toy maze environment illustrating the confounding policy update problem.

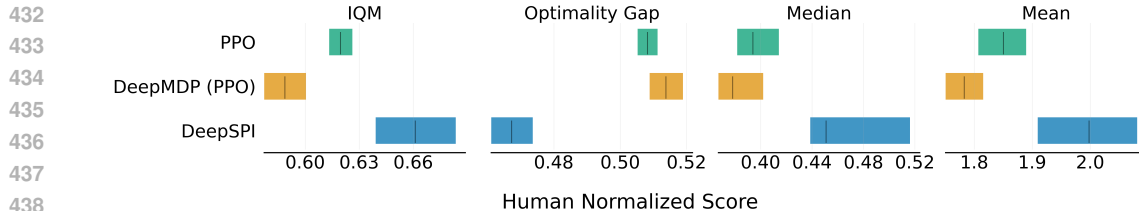


Figure 5: Aggregate results on stochastic versions of the standard 57 environments from ALE, with 95% confidence intervals (CIs). Higher values for the mean, median, and *interquartile mean* (IQM) indicate better performance, while a lower optimality gap is preferable (cf. Agarwal et al. 2021b). CIs are obtained through percentile bootstrapping with stratified resampling. Plots per environment available in Appendix H.2.

Appendix G). To improve upon the policy that always chooses “right,” the agent must learn to assign distinct representations to the two \star cells, select “up” in the top one, and “right” in the bottom one.

We compare the behaviour of PPO and DeepSPI in this environment. Since our goal is to highlight the agent’s representation-learning capabilities, each observation is provided as raw pixels. The agent must therefore learn both a policy and an encoder mapping pixels to a structured latent space. Further details on the environment and observation scheme are given in Appendix G. As shown in Fig. 4, the representation learned by PPO collapses the top and bottom \star cells into a single latent state. With such a representation, the best policy PPO can learn is to always choose “right,” which leads to a return of ~ 4.8 . In contrast, DeepSPI benefits from the representation quality guarantees of Thm. 4, which ensure that states with different values remain separated in the latent space for all policies in a suitable neighborhood. This is exactly what we observe: the learned representation distinguishes the two \star cells. As a result, the agent learns to choose “up” in the top \star cell and “right” in the bottom one, achieving a return of ~ 8 .

7 EXPERIMENTS

In this section, we evaluate the practical performance of DeepSPI in environments where (i) representation learning is essential and (ii) dynamics are complex. We use the Atari Arcade Learning Environment (ALE; Bellemare et al. 2013) and consider each state as four stacked frames. ALE domains feature a wide range of dynamics; to further introduce stochasticity, we follow Machado et al. (2018) and employ two standard tricks: *sticky actions*, where with probability p_a the previous action is repeated (simulating joystick or reaction-time imperfections), and *random initialisation*, where the agent begins after n_{NOOP} initial no-op frames. We set $p_a = 0.3$ and $n_{\text{NOOP}} = 60$.

As baselines, we consider PPO (vectorized cleanRL implementation; Huang et al., 2022) and DeepMDPs (Gelada et al., 2019). Essentially, DeepMDPs are principled auxiliary tasks (the losses L_R, L_P presented in Sect. 5) that can be plugged to any RL algorithm to improve the representation learned (with guarantees). The main difference with DeepSPI is that L_R, L_P are able to push the updated policy out of the neighborhood by learning the representation via the additional losses, for which updates are not constrained. This means that *none of the SPI guarantees presented in this paper apply* to DeepMDPs. For a fair comparison, we plugged the DeepMDP losses to (vectorized) PPO, and we use the architecture as for DeepSPI. We use the default cleanRL’s hyperparameters for the three algorithms, except for the data collection (128 environments with a horizon of 8 steps).

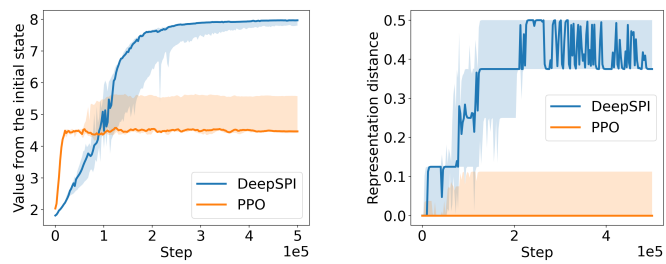


Figure 4: Value from cell I in the maze (left) and distance between the representation of the \star cell from the top and bottom branches (right).

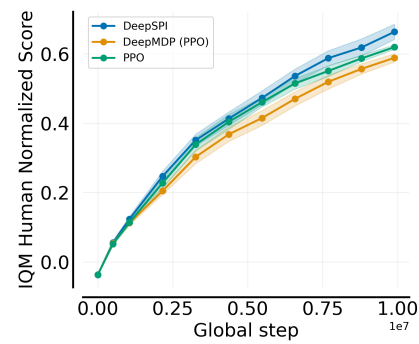


Figure 6: Sample efficiency w.r.t. IQM normalized scores on the stochastic ALE-57. Shaded regions give pointwise 95% CIs obtained via percentile stratified bootstrap.

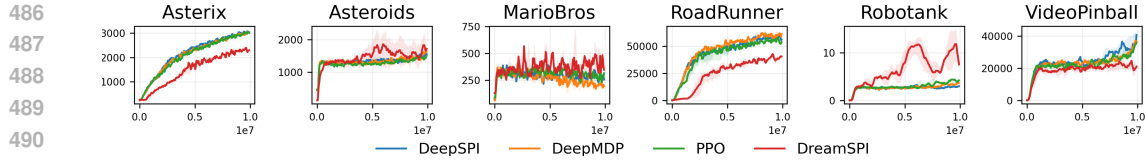


Figure 8: Sample environments from ALE where DreamSPI learns meaningful behaviors.

As latent space, we use the raw 3D representation obtained after the convolution layers (as recommended and used by Gelada et al., 2019). For modeling the transition function, we found best to use a mixture of multivariate normal distributions (the transition network outputs 5 means/diagonal matrices). **To deal with the Lipschitz constraints that need to be enforced on the reward and transition functions, we found the most efficient to model \bar{R}, \bar{P} via Lipschitz networks (precisely, we use norm-constrained GroupSort architectures to enforce 1-Lipschitzness; Anil et al., 2019).**

As shown in Fig. 5 and 6, DeepSPI delivers strong performance, improving on both PPO and DeepMDP. Notably, these results are obtained while preserving SPI-style properties; a valuable combination, as such theoretical control typically comes at the expense of performance and substantial data requirements.

Beyond pure performance, we want to assess whether the world model, learned via DeepSPI, exhibits accurate dynamics.

Fig. 7 reports L_P, L_R during training. Note that DeepSPI consistently achieves lower transition losses, indicating more accurate transition functions. **We discuss the statistical significance of that statement in Appendix H.2.** In contrast to the off-policy setting where Gelada et al. (2019) reported competing transition and reward losses, we did not observe such behavior in our parallel on-policy setting. We attribute this stability to the fact that our losses are always computed under the current policy, unlike off-policy methods that rely on replay buffers.

To probe the predictive quality of the latent model and illustrate Thm. 3, we introduced DreamSPI, a naïve variant where DeepSPI learns the world model and representation, and PPO updates the policy *from imagined trajectories* (Appendix F). Unlike off-policy approaches that exploit replay buffers and update the model at every interaction step, our fully on-policy setting updates the world model only from fresh interaction data, which makes combining model learning and planning inherently more challenging. Even so, DreamSPI achieves learning progress in several environments and exhibits coherent behaviours (cf. Fig. 8 & Appendix H.2). While its aggregate median score remains below the baselines, this is somehow expected given the stricter data requirements compared to usual model-based approaches. Importantly, the ability to maintain a model offers benefits that extend far beyond raw scores, enabling future applications in safety, verification, and reactive synthesis.

8 CONCLUSION AND FUTURE WORK

We developed a theoretical framework for safe policy improvement (SPI) that combines world-model and representation learning in nontrivial settings. Our results show that constraining policy updates within a well-defined neighborhood yields monotonic improvement and convergence, while auxiliary transition and reward losses ensure that the latent space remains suitable for policy optimisation. We further provided model-quality guarantees in the form of a “deep” SPI theorem, which jointly accounts for the learned representation and the reward/transition losses. These results directly address two critical issues in model-based RL: out-of-trajectory errors and confounding policy updates. Building on this analysis, we proposed DeepSPI, a principled algorithm that integrates the theoretical ingredients with PPO. On ALE, DeepSPI is competitive with and often improves upon PPO and DeepMDPs, while providing SPI guarantees.

This work opens several directions. A first avenue is to make pure deep SPI model-based planning practical. Our experiments with DreamSPI suggest that this is feasible but requires improved sample efficiency. Another direction goes beyond return optimization: a principled world model, grounded in our theory, can support safe reinforcement learning via formal methods, through synthesis (Delgrange et al., 2025; Lechner et al., 2022), or shielding (Jansen et al., 2020).

Figure 7: Median transition and reward losses during training, aggregated across all the ALE. For the sake of visualization, we cut L_P lower values from the plot.

540 REPRODUCIBILITY STATEMENT
541

542 All theoretical results are stated with explicit assumptions, and complete proofs are included in the
543 appendix. The experimental setup is described in detail in the main text and supplementary material,
544 including environments, hyperparameters, and training procedures. We provide the full source code
545 as supplementary material to enable reproduction of our results. Datasets used in the experiments are
546 publicly available (we use envpool Atari).

548 REFERENCES
549

550 Rishabh Agarwal, Marlos C. Machado, Pablo Samuel Castro, and Marc G. Bellemare. Contrastive
551 behavioral similarity embeddings for generalization in reinforcement learning. In *9th International
552 Conference on Learning Representations, ICLR 2021, Virtual Event, Austria, May 3-7, 2021.*
553 OpenReview.net, 2021a.

554 Rishabh Agarwal, Max Schwarzer, Pablo Samuel Castro, Aaron C. Courville, and Marc G. Bellemare.
555 Deep reinforcement learning at the edge of the statistical precipice. In Marc'Aurelio
556 Ranzato, Alina Beygelzimer, Yann N. Dauphin, Percy Liang, and Jennifer Wortman Vaughan,
557 editors, *Advances in Neural Information Processing Systems 34: Annual Conference on Neu-
558 ral Information Processing Systems 2021, NeurIPS 2021, December 6-14, 2021, virtual,*
559 pages 29304–29320, 2021b. URL [https://proceedings.neurips.cc/paper/2021/
560 hash/f514cec81cb148559cf475e7426eed5e-Abstract.html](https://proceedings.neurips.cc/paper/2021/hash/f514cec81cb148559cf475e7426eed5e-Abstract.html).

561 Lucas Nunes Alegre, Ana L. C. Bazzan, Diederik M. Roijers, Ann Nowé, and Bruno C. da Silva.
562 Sample-efficient multi-objective learning via generalized policy improvement prioritization. In
563 Noa Agmon, Bo An, Alessandro Ricci, and William Yeoh, editors, *Proceedings of the 2023
564 International Conference on Autonomous Agents and Multiagent Systems, AAMAS 2023, London,
565 United Kingdom, 29 May 2023 - 2 June 2023*, pages 2003–2012. ACM, 2023. doi: 10.5555/
566 3545946.3598872. URL <https://dl.acm.org/doi/10.5555/3545946.3598872>.

567 Cem Anil, James Lucas, and Roger B. Grosse. Sorting out lipschitz function approximation. In
568 Kamalika Chaudhuri and Ruslan Salakhutdinov, editors, *Proceedings of the 36th International
569 Conference on Machine Learning, ICML 2019, 9-15 June 2019, Long Beach, California, USA,*
570 volume 97 of *Proceedings of Machine Learning Research*, pages 291–301. PMLR, 2019. URL
571 <http://proceedings.mlr.press/v97/anil19a.html>.

572 Raphaël Avalos, Florent Delgrange, Ann Nowe, Guillermo Perez, and Diederik M Roijers. The
573 wasserstein believer: Learning belief updates for partially observable environments through reliable
574 latent space models. In *The Twelfth International Conference on Learning Representations*, 2024.
575 URL <https://openreview.net/forum?id=KrtGfTGaGe>.

577 M. G. Bellemare, Y. Naddaf, J. Veness, and M. Bowling. The arcade learning environment: An
578 evaluation platform for general agents. *Journal of Artificial Intelligence Research*, 47:253–279,
579 jun 2013.

581 Richard Bellman. *Dynamic Programming*. Dover Publications, 1957. ISBN 9780486428093.

582 Jacob Buckman, Danijar Hafner, G. Tucker, Eugene Brevdo, and Honglak Lee. Sample-efficient
583 reinforcement learning with stochastic ensemble value expansion. *ArXiv*, abs/1807.01675, 2018.
584 URL <https://api.semanticscholar.org/CorpusID:49577255>.

585 Alberto Castellini, Federico Bianchi, Edoardo Zorzi, Thiago D. Simão, Alessandro Farinelli, and
586 Matthijs T. J. Spaan. Scalable safe policy improvement via Monte Carlo tree search. In Andreas
587 Krause, Emma Brunskill, Kyunghyun Cho, Barbara Engelhardt, Sivan Sabato, and Jonathan
588 Scarlett, editors, *Proceedings of the 40th International Conference on Machine Learning*, volume
589 202 of *Proceedings of Machine Learning Research*, pages 3732–3756. PMLR, 23–29 Jul 2023.
590 URL <https://proceedings.mlr.press/v202/castellini23a.html>.

592 Pablo Samuel Castro. Scalable methods for computing state similarity in deterministic Markov
593 Decision Processes. In *Proceedings of the Thirty-Fourth AAAI Conference on Artificial Intelligence
(AAAI-20)*, 2020.

594 Pablo Samuel Castro, Tyler Kastner, Prakash Panangaden, and Mark Rowland. MICO: Improved
 595 representations via sampling-based state similarity for Markov decision processes. In M. Ranzato,
 596 A. Beygelzimer, Y. Dauphin, P.S. Liang, and J. Wortman Vaughan, editors, *Advances in Neural
 597 Information Processing Systems*, volume 34, pages 30113–30126. Curran Associates, Inc., 2021.
 598

599 Florent Delgrange, Ann Nowé, and Guillermo A. Pérez. Distillation of rl policies with formal
 600 guarantees via variational abstraction of markov decision processes. *Proceedings of the AAAI
 601 Conference on Artificial Intelligence*, 36(6):6497–6505, Jun. 2022. doi: 10.1609/aaai.v36i6.20602.

602 Florent Delgrange, Guy Avni, Anna Lukina, Christian Schilling, Ann Nowe, and Guillermo Perez.
 603 Composing reinforcement learning policies, with formal guarantees. In *Proceedings of the 24th
 604 International Conference on Autonomous Agents and Multiagent Systems, AAMAS 2025, Detroit,
 605 Michigan, USA, May 19-23, IFAAMAS*, 2025.

606 Josée Desharnais, Abbas Edalat, and Prakash Panangaden. A logical characterization of bisimulation
 607 for labeled markov processes. In *Thirteenth Annual IEEE Symposium on Logic in Computer Science,
 608 Indianapolis, Indiana, USA, June 21-24, 1998*, pages 478–487. IEEE Computer Society, 1998. doi:
 609 10.1109/LICS.1998.705681. URL <https://doi.org/10.1109/LICS.1998.705681>.
 610

611 Kefan Dong, Yannis Flet-Berliac, Allen Nie, and Emma Brunskill. Model-based offline reinforcement
 612 learning with local misspecification. In Brian Williams, Yiling Chen, and Jennifer Neville, editors,
 613 *Thirty-Seventh AAAI Conference on Artificial Intelligence, AAAI 2023, Thirty-Fifth Conference on
 614 Innovative Applications of Artificial Intelligence, IAAI 2023, Thirteenth Symposium on Educational
 615 Advances in Artificial Intelligence, EAAI 2023, Washington, DC, USA, February 7-14, 2023*, pages
 616 7423–7431. AAAI Press, 2023. doi: 10.1609/AAAI.V37I6.25903. URL <https://doi.org/10.1609/aaai.v37i6.25903>.
 617

618 Ayoub Echchahed and Pablo Samuel Castro. A survey of state representation learning for deep
 619 reinforcement learning. 2025, 2025.

620 Norm Ferns, Prakash Panangaden, and Doina Precup. Bisimulation metrics for continuous markov
 621 decision processes. *SIAM J. Comput.*, 40(6):1662–1714, 2011. doi: 10.1137/10080484X. URL
 622 <https://doi.org/10.1137/10080484X>.
 623

624 Vincent François-Lavet, Yoshua Bengio, Doina Precup, and Joelle Pineau. Combined reinforcement
 625 learning via abstract representations. In *The Thirty-Third AAAI Conference on Artificial Intelligence,
 626 AAAI 2019, The Thirty-First Innovative Applications of Artificial Intelligence Conference, IAAI
 627 2019, The Ninth AAAI Symposium on Educational Advances in Artificial Intelligence, EAAI
 628 2019, Honolulu, Hawaii, USA, January 27 - February 1, 2019*, pages 3582–3589. AAAI Press,
 629 2019. doi: 10.1609/AAAI.V33I01.33013582. URL <https://doi.org/10.1609/aaai.v33i01.33013582>.
 630

631 Matteo Gallici, Mattie Fellows, Benjamin Ellis, Bartomeu Pou, Ivan Masmitja, Jakob Nicolaus
 632 Foerster, and Mario Martin. Simplifying deep temporal difference learning. In *The Thirteenth
 633 International Conference on Learning Representations*, 2025. URL <https://openreview.net/forum?id=7IzeL0kflu>.
 634

635 Matthieu Geist, Bruno Scherrer, and Olivier Pietquin. A theory of regularized markov decision
 636 processes. In Kamalika Chaudhuri and Ruslan Salakhutdinov, editors, *Proceedings of the 36th
 637 International Conference on Machine Learning, ICML 2019, 9-15 June 2019, Long Beach, Califor-
 638 nia, USA*, volume 97 of *Proceedings of Machine Learning Research*, pages 2160–2169. PMLR,
 639 2019. URL <http://proceedings.mlr.press/v97/geist19a.html>.
 640

641 Carles Gelada, Saurabh Kumar, Jacob Buckman, Ofir Nachum, and Marc G. Bellemare. Deepmdp:
 642 Learning continuous latent space models for representation learning. In Kamalika Chaudhuri
 643 and Ruslan Salakhutdinov, editors, *Proceedings of the 36th International Conference on Machine
 644 Learning, ICML 2019, 9-15 June 2019, Long Beach, California, USA*, volume 97 of *Proceedings
 645 of Machine Learning Research*, pages 2170–2179. PMLR, 2019.

646 Mohammad Ghavamzadeh, Marek Petrik, and Yinlam Chow. Safe policy improvement by minimizing
 647 robust baseline regret. In Daniel D. Lee, Masashi Sugiyama, Ulrike von Luxburg, Isabelle Guyon,
 and Roman Garnett, editors, *Advances in Neural Information Processing Systems 29: Annual*

648 *Conference on Neural Information Processing Systems 2016, December 5-10, 2016, Barcelona,*
 649 *Spain*, pages 2298–2306, 2016a. URL <https://proceedings.neurips.cc/paper/2016/hash/9a3d458322d70046f63dfd8b0153ece4-Abstract.html>.

650

651 Mohammad Ghavamzadeh, Marek Petrik, and Yinlam Chow. Safe policy improvement by mini-
 652 mizing robust baseline regret. In D. Lee, M. Sugiyama, U. Luxburg, I. Guyon, and R. Garnett,
 653 editors, *Advances in Neural Information Processing Systems*, volume 29. Curran Associates, Inc.,
 654 2016b. URL https://proceedings.neurips.cc/paper_files/paper/2016/file/9a3d458322d70046f63dfd8b0153ece4-Paper.pdf.

655

656

657 Robert Givan, Thomas L. Dean, and Matthew Greig. Equivalence notions and model minimization in
 658 markov decision processes. *Artif. Intell.*, 147(1-2):163–223, 2003. doi: 10.1016/S0004-3702(02)
 659 00376-4. URL [https://doi.org/10.1016/S0004-3702\(02\)00376-4](https://doi.org/10.1016/S0004-3702(02)00376-4).

660

661 Ishaan Gulrajani, Faruk Ahmed, Martin Arjovsky, Vincent Dumoulin, and Aaron C
 662 Courville. Improved training of wasserstein gans. In I. Guyon, U. Von Luxburg,
 663 S. Bengio, H. Wallach, R. Fergus, S. Vishwanathan, and R. Garnett, editors, *Ad-*
 664 *vances in Neural Information Processing Systems*, volume 30. Curran Associates, Inc.,
 665 2017. URL https://proceedings.neurips.cc/paper_files/paper/2017/file/892c3b1c6dccc52936e27cbd0ff683d6-Paper.pdf.

666

667 David Ha and Jürgen Schmidhuber. World models. *CoRR*, abs/1803.10122, 2018. URL <http://arxiv.org/abs/1803.10122>.

668

669 Danijar Hafner, Timothy P. Lillicrap, Mohammad Norouzi, and Jimmy Ba. Mastering atari with
 670 discrete world models. In *9th International Conference on Learning Representations, ICLR 2021,*
 671 *Virtual Event, Austria, May 3-7, 2021*. OpenReview.net, 2021. URL <https://openreview.net/forum?id=0oabwyZbOu>.

672

673 Wassily Hoeffding. Probability inequalities for sums of bounded random variables. *Journal of*
 674 *the American Statistical Association*, 58(301):13–30, 1963. ISSN 01621459. URL <http://www.jstor.org/stable/2282952>.

675

676 Bojun Huang. Steady state analysis of episodic reinforcement learning. In Hugo Larochelle,
 677 Marc’Aurelio Ranzato, Raia Hadsell, Maria-Florina Balcan, and Hsuan-Tien Lin, editors, *Ad-*
 678 *vances in Neural Information Processing Systems 33: Annual Conference on Neural Information*
 679 *Processing Systems 2020, NeurIPS 2020, December 6-12, 2020, virtual*, 2020.

680

681 Shengyi Huang, Rousslan Fernand Julien Dossa, Chang Ye, Jeff Braga, Dipam Chakraborty, Kinal
 682 Mehta, and João G.M. Araújo. Cleanrl: High-quality single-file implementations of deep rein-
 683 forcement learning algorithms. *Journal of Machine Learning Research*, 23(274):1–18, 2022. URL
 684 <http://jmlr.org/papers/v23/21-1342.html>.

685

686 Garud N. Iyengar. Robust dynamic programming. *Math. Oper. Res.*, 30(2):257–280, 2005. doi:
 687 10.1287/MOOR.1040.0129. URL <https://doi.org/10.1287/moor.1040.0129>.

688 Nils Jansen, Bettina Könighofer, Sebastian Junges, Alex Serban, and Roderick Bloem. Safe rein-
 689 forcement learning using probabilistic shields (invited paper). In Igor Konnov and Laura Kovács,
 690 editors, *31st International Conference on Concurrency Theory, CONCUR 2020, September 1-*
 691 *4, 2020, Vienna, Austria (Virtual Conference)*, volume 171 of *LIPICS*, pages 3:1–3:16. Schloss
 692 Dagstuhl - Leibniz-Zentrum für Informatik, 2020. doi: 10.4230/LIPICS.CONCUR.2020.3. URL
 693 <https://doi.org/10.4230/LIPICS.CONCUR.2020.3>.

694 J. L. W. V. Jensen. Sur les fonctions convexes et les inégalités entre les valeurs moyennes. *Acta*
 695 *Mathematica*, 30:175–193, 1906.

696 Leonid Kantorovich and Gennady S. Rubinstein. On a space of totally additive functions. *Vestnik*
 697 *Leningrad. Univ.*, 13:52–59, 1958.

698

699 Rahul Kidambi, Aravind Rajeswaran, Praneeth Netrapalli, and Thorsten Joachims. Morel: Model-
 700 based offline reinforcement learning. In Hugo Larochelle, Marc’Aurelio Ranzato, Raia Hadsell,
 701 Maria-Florina Balcan, and Hsuan-Tien Lin, editors, *Advances in Neural Information Processing*
 702 *Systems 33: Annual Conference on Neural Information Processing Systems 2020, NeurIPS 2020*,

702 *December 6-12, 2020, virtual*, 2020. URL <https://proceedings.neurips.cc/paper/2020/hash/f7efa4f864ae9b88d43527f4b14f750f-Abstract.html>.

703

704

705 Jakub Grudzien Kuba, Christian A. Schröder de Witt, and Jakob N. Foerster. Mirror learning: A
706 unifying framework of policy optimisation. In Kamalika Chaudhuri, Stefanie Jegelka, Le Song,
707 Csaba Szepesvári, Gang Niu, and Sivan Sabato, editors, *International Conference on Machine
708 Learning, ICML 2022, 17-23 July 2022, Baltimore, Maryland, USA*, volume 162 of *Proceedings of
709 Machine Learning Research*, pages 7825–7844. PMLR, 2022.

710

711 Romain Laroche, Paul Trichelair, and Remi Tachet Des Combes. Safe policy improvement with
712 baseline bootstrapping. In Kamalika Chaudhuri and Ruslan Salakhutdinov, editors, *Proceedings of
713 the 36th International Conference on Machine Learning*, volume 97 of *Proceedings of Machine
714 Learning Research*, pages 3652–3661. PMLR, 09–15 Jun 2019. URL <https://proceedings.mlr.press/v97/laroche19a.html>.

715

716 Kim Guldstrand Larsen and Arne Skou. Bisimulation through probabilistic testing. *Inf. Comput.*, 94
717 (1):1–28, 1991. doi: 10.1016/0890-5401(91)90030-6. URL [https://doi.org/10.1016/0890-5401\(91\)90030-6](https://doi.org/10.1016/0890-5401(91)90030-6).

718

719 Mathias Lechner, Dorde Zikelic, Krishnendu Chatterjee, and Thomas A. Henzinger. Stability ver-
720 ification in stochastic control systems via neural network supermartingales. In *Thirty-Sixth
721 AAAI Conference on Artificial Intelligence, AAAI 2022, Thirty-Fourth Conference on Inno-
722 vative Applications of Artificial Intelligence, IAAI 2022, The Twelfth Symposium on Edu-
723 cational Advances in Artificial Intelligence, EAAI 2022 Virtual Event, February 22 - March
724 1, 2022*, pages 7326–7336. AAAI Press, 2022. doi: 10.1609/AAAI.V36I7.20695. URL
725 <https://doi.org/10.1609/aaai.v36i7.20695>.

726

727 Lihong Li, Thomas J. Walsh, and Michael L. Littman. Towards a unified theory of state abstraction
728 for mdps. In *International Symposium on Artificial Intelligence and Mathematics, AI&Math 2006,
729 Fort Lauderdale, Florida, USA, January 4-6, 2006*, 2006. URL <http://anytime.cs.umass.edu/aimath06/proceedings/P21.pdf>.

730

731 Marlos C. Machado, Marc G. Bellemare, Erik Talvitie, Joel Veness, Matthew J. Hausknecht, and
732 Michael Bowling. Revisiting the arcade learning environment: Evaluation protocols and open
733 problems for general agents. *Journal of Artificial Intelligence Research*, 61:523–562, 2018.

734

735 Walter Mayor, Johan Obando-Ceron, Aaron Courville, and Pablo Samuel Castro. The impact of
736 on-policy parallelized data collection on deep reinforcement learning networks. In *Forty-second
737 International Conference on Machine Learning*, 2025. URL <https://openreview.net/forum?id=cnqyzuZhSo>.

738

739 Alberto Maria Metelli, Mirco Mutti, and Marcello Restelli. A tale of sampling and estimation in
740 discounted reinforcement learning. In Francisco J. R. Ruiz, Jennifer G. Dy, and Jan-Willem van de
741 Meent, editors, *International Conference on Artificial Intelligence and Statistics, 25-27 April
742 2023, Palau de Congressos, Valencia, Spain*, volume 206 of *Proceedings of Machine Learning
743 Research*, pages 4575–4601. PMLR, 2023. URL <https://proceedings.mlr.press/v206/metelli23a.html>.

744

745 Gaspard Monge. Mémoire sur la théorie des déblais et des remblais. In *Histoire de l'Académie
746 royale des sciences avec les mémoires de mathématique et de physique tirés des registres de cette
747 Académie*, pages 666 – 705. 1781.

748

749 Alfred Müller. Integral probability metrics and their generating classes of functions. *Advances in
750 Applied Probability*, 29(2):429–443, 1997. ISSN 00018678. URL <http://www.jstor.org/stable/1428011>.

751

752 Arnab Nilim and Laurent El Ghaoui. Robust control of markov decision processes with uncertain
753 transition matrices. *Oper. Res.*, 53(5):780–798, 2005. doi: 10.1287/OPRE.1050.0216. URL
754 <https://doi.org/10.1287/opre.1050.0216>.

755

756 Efe A. Ok. *Real Analysis with Economic Applications*. Princeton University Press, 2007. ISBN
757 9780691117683.

756 Martin L. Puterman. *Markov Decision Processes: Discrete Stochastic Dynamic Programming*.
 757 Wiley Series in Probability and Statistics. Wiley, 1994. ISBN 978-0-47161977-2. doi: 10.1002/
 758 9780470316887. URL <https://doi.org/10.1002/9780470316887>.

759

760 D. Revuz. *Markov Chains*. North-Holland mathematical library. Elsevier Science Publishers B.V.,
 761 second (revised) edition, 1984. ISBN 9780444864000.

762

763 Julian Schrittwieser, Ioannis Antonoglou, Thomas Hubert, Karen Simonyan, Laurent Sifre, Simon
 764 Schmitt, Arthur Guez, Edward Lockhart, Demis Hassabis, Thore Graepel, Timothy Lillicrap, and
 765 David Silver. Mastering Atari, Go, chess and shogi by planning with a learned model. *Nature*, 588
 766 (7839):604–609, 2020. doi: 10.1038/s41586-020-03051-4.

767

768 John Schulman, Sergey Levine, Pieter Abbeel, Michael I. Jordan, and Philipp Moritz. Trust region
 769 policy optimization. In Francis R. Bach and David M. Blei, editors, *Proceedings of the 32nd*
 770 *International Conference on Machine Learning, ICML 2015, Lille, France, 6-11 July 2015*,
 771 volume 37 of *JMLR Workshop and Conference Proceedings*, pages 1889–1897. JMLR.org, 2015.
 772 URL <http://proceedings.mlr.press/v37/schulman15.html>.

773

774 John Schulman, Filip Wolski, Prafulla Dhariwal, Alec Radford, and Oleg Klimov. Proximal policy
 775 optimization algorithms. *CoRR*, abs/1707.06347, 2017.

776

777 R. Serfozo. *Basics of Applied Stochastic Processes*. Probability and Its Applications. Springer Berlin
 778 Heidelberg, 2009. ISBN 9783540893325.

779

780 Thiago D. Simão, Romain Laroche, and Rémi Tachet des Combes. Safe policy improvement with
 781 an estimated baseline policy. In Amal El Fallah Seghrouchni, Gita Sukthankar, Bo An, and Neil
 782 Yorke-Smith, editors, *Proceedings of the 19th International Conference on Autonomous Agents*
 783 *and Multiagent Systems, AAMAS '20, Auckland, New Zealand, May 9-13, 2020*, pages 1269–1277.
 784 International Foundation for Autonomous Agents and Multiagent Systems, 2020. doi: 10.5555/
 785 3398761.3398908. URL <https://dl.acm.org/doi/10.5555/3398761.3398908>.

786

787 Elias M. Stein and Rami Shakarchi. *Real Analysis: Measure Theory, Integration, and Hilbert Spaces*.
 788 Princeton University Press, 2005. ISBN 9780691113869.

789

790 Miguel Suau, Matthijs T. J. Spaan, and Frans A. Oliehoek. Bad Habits: Policy Confounding and
 791 Out-of-Trajectory Generalization in RL. *RLJ*, 4:1711–1732, 2024.

792

793 Marnix Suilen, Thom S. Badings, Eline M. Bovy, David Parker, and Nils Jansen. Robust markov
 794 decision processes: A place where AI and formal methods meet. In Nils Jansen, Sebastian Junges,
 795 Benjamin Lucien Kaminski, Christoph Matheja, Thomas Noll, Tim Quatmann, Mariëlle Stoelinga,
 796 and Matthias Volk, editors, *Principles of Verification: Cycling the Probabilistic Landscape -*
 797 *Essays Dedicated to Joost-Pieter Katoen on the Occasion of His 60th Birthday, Part III*, volume
 798 15262 of *Lecture Notes in Computer Science*, pages 126–154. Springer, 2024. doi: 10.1007/
 799 978-3-031-75778-5_7. URL https://doi.org/10.1007/978-3-031-75778-5_7.

800

801 Richard S. Sutton and Andrew G. Barto. *Reinforcement learning - an introduction*, 2nd Edition. MIT
 802 Press, 2018.

803

804 Philip S. Thomas, Georgios Theocharous, and Mohammad Ghavamzadeh. High confidence policy
 805 improvement. In Francis R. Bach and David M. Blei, editors, *Proceedings of the 32nd International*
 806 *Conference on Machine Learning, ICML 2015, Lille, France, 6-11 July 2015*, volume 37 of
 807 *JMLR Workshop and Conference Proceedings*, pages 2380–2388. JMLR.org, 2015. URL <http://proceedings.mlr.press/v37/thomas15.html>.

808

809 Elise van der Pol, Thomas Kipf, Frans A. Oliehoek, and Max Welling. Plannable approximations to
 810 MDP homomorphisms: Equivariance under actions. In Amal El Fallah Seghrouchni, Gita Suk-
 811 thankar, Bo An, and Neil Yorke-Smith, editors, *Proceedings of the 19th International Conference*
 812 *on Autonomous Agents and Multiagent Systems, AAMAS '20, Auckland, New Zealand, May 9-13,*
 813 *2020*, pages 1431–1439. International Foundation for Autonomous Agents and Multiagent Sys-
 814 tems, 2020. doi: 10.5555/3398761.3398926. URL <https://dl.acm.org/doi/10.5555/3398761.3398926>.

810 Robert J. Vanderbei. Uniform continuity is almost Lipschitz continuity. Technical Report SOR-91-11,
 811 Statistics and Operations Research Series, Princeton University, 1991.
 812

813 Leonid Nisonovich Vaserstein. Markov processes over denumerable products of spaces, describing
 814 large systems of automata. *Problemy Peredaci Informacii*, 5:64–72, 1969.

815 Cédric Villani. *The Wasserstein distances*, pages 93–111. Springer Berlin Heidelberg, Berlin,
 816 Heidelberg, 2009. ISBN 978-3-540-71050-9. doi: 10.1007/978-3-540-71050-9_6. URL https://doi.org/10.1007/978-3-540-71050-9_6.

816

817 Patrick Wienhöft, Marnix Suilen, Thiago D. Simão, Clemens Dubslaff, Christel Baier, and Nils Jansen.
 818 More for less: Safe policy improvement with stronger performance guarantees. In *Proceedings of
 819 the Thirty-Second International Joint Conference on Artificial Intelligence, IJCAI 2023, 19th-25th
 820 August 2023, Macao, SAR, China*, pages 4406–4415. ijcai.org, 2023. doi: 10.24963/IJCAI.2023/
 821 490. URL <https://doi.org/10.24963/ijcai.2023/490>.

822

823

824 Wolfram Wiesemann, Daniel Kuhn, and Berç Rustem. Robust markov decision processes. *Math.
 825 Oper. Res.*, 38(1):153–183, 2013. doi: 10.1287/MOOR.1120.0566. URL <https://doi.org/10.1287/moor.1120.0566>.

826

827 Frank Wilcoxon. *Individual Comparisons by Ranking Methods*, pages 196–202. Springer New York,
 828 New York, NY, 1992. ISBN 978-1-4612-4380-9. doi: 10.1007/978-1-4612-4380-9_16. URL
 829 https://doi.org/10.1007/978-1-4612-4380-9_16.

830

831 Chenjun Xiao, Yifan Wu, Chen Ma, Dale Schuurmans, and Martin Müller. Learning to combat
 832 compounding-error in model-based reinforcement learning. *CoRR*, abs/1912.11206, 2019.

833

834 Tianhe Yu, Garrett Thomas, Lantao Yu, Stefano Ermon, James Y. Zou, Sergey Levine,
 835 Chelsea Finn, and Tengyu Ma. MOPO: model-based offline policy optimization. In
 836 Hugo Larochelle, Marc'Aurelio Ranzato, Raia Hadsell, Maria-Florina Balcan, and Hsuan-
 837 Tien Lin, editors, *Advances in Neural Information Processing Systems 33: Annual Con-
 838 ference on Neural Information Processing Systems 2020, NeurIPS 2020, December 6-12,
 839 2020, virtual*, 2020. URL <https://proceedings.neurips.cc/paper/2020/hash/a322852ce0df73e204b7e67cbbef0d0a-Abstract.html>.

840

841 Tianhe Yu, Aviral Kumar, Rafael Rafailov, Aravind Rajeswaran, Sergey Levine, and Chelsea
 842 Finn. COMBO: conservative offline model-based policy optimization. In Marc'Aurelio Ran-
 843 zato, Alina Beygelzimer, Yann N. Dauphin, Percy Liang, and Jennifer Wortman Vaughan,
 844 editors, *Advances in Neural Information Processing Systems 34: Annual Conference on Neural
 845 Information Processing Systems 2021, NeurIPS 2021, December 6-14, 2021, virtual*, pages
 846 28954–28967, 2021. URL <https://proceedings.neurips.cc/paper/2021/hash/f29a179746902e331572c483c45e5086-Abstract.html>.

847

848 Amy Zhang, Rowan Thomas McAllister, Roberto Calandra, Yarin Gal, and Sergey Levine. Learning
 849 invariant representations for reinforcement learning without reconstruction. In *International
 850 Conference on Learning Representations*, 2021. URL <https://openreview.net/forum?id=-2FCwDKRREu>.

851

852

853

854

855

856

857

858

859

860

861

862

863

864 **Appendix**
 865
 866

867 **A REMARK ON VALUE FUNCTIONS AND EPISODIC PROCESSES**
 868

869 An *episodic process* is formally defined as an MDP $\mathcal{M} = \langle \mathcal{S}, \mathcal{A}, P, R, s_I, \gamma \rangle$ where:
 870

- 871 (i) there is a special state $s_{reset} \in \mathcal{S}$, intuitively indicating the termination of any *episode*;
- 872 (ii) the reset state does not incur any reward: $R(s_{reset}, a) = 0$ for all actions $a \in \mathcal{A}$;
- 873 (iii) s_{reset} is almost surely visited under any policy: for all policies $\pi \in \Pi$, $\mathbb{P}_\pi \left(\left\{ (s_t, a_t)_{t \geq 0} \mid \exists i: s_i = s_{reset} \right\} \right) = 1$;
 875 and
- 876 (iv) \mathcal{M} restarts from the initial state once reset: $P(\{s_I\} \mid s_{reset}, a) = 1$ for all $a \in \mathcal{A}$.
 877

878 Note that by items (iii) and (iv), s_{reset} is almost surely **infinitely often** visited: we have for all $\pi \in \Pi$ that
 879

$$880 \mathbb{P}_\pi \left(\left\{ (s_t, a_t)_{t \geq 0} \mid \forall i \geq 0, \exists j > i: s_j = s_{reset} \right\} \right) = 1. \\ 881$$

882 Alternatively and equivalently, an episodic process may also be defined without a unique reset state by the means of
 883 several *terminal states*, which go back to the initial state with probability one.

884 An *episode* of \mathcal{M} is thus the prefix $s_0, a_0, \dots, a_{t-1}, s_t$ of a trajectory where $s_t = s_{reset}$ and for all $i < t$, $s_i \neq s_{reset}$.
 885 Notice that our formulation embeds (but is not limited to) finite-horizon tasks, where an upper bound on the length
 886 of the episodes is fixed. The *average episode length* (AEL) of π is then formally defined as $\text{AEL}(\pi) = \mathbb{E}_\pi [\mathbf{T}]$ with
 887

$$888 \mathbf{T}(\tau) = \sum_{i=0}^{\infty} (i+1) \cdot \mathbb{1} \{ s_i = s_{reset} \text{ and } \forall j < i, s_j \neq s_{reset} \} \\ 889 \\ 890$$

891 for any trajectory $\tau = (s_t, a_t)_{t \geq 0}$.
 892

893 Often, when considering episodic tasks, RL algorithms stops accumulating rewards upon the termination of every
 894 episode. In practical implementations, this corresponds to discarding rewards when a flag `done`, indicating episode
 895 termination, is set to `true`. In such case, we may slightly adapt our value functions as:
 896

$$897 V^\pi(s) = \begin{cases} \mathbb{E}_\pi \left[\sum_{t=0}^{\infty} \left(\prod_{i=1}^t \mathbb{1} \{ s_i \neq s_{reset} \} \cdot \gamma \right) R(s_t, a_t) \mid s_0 = s \right] & \text{if } s \neq s_{reset} \\ 0 & \text{otherwise;} \end{cases} \\ 898 \\ 899$$

900 or, when formalized as Bellman's equation:
 901

$$902 Q^\pi(s, a) = \begin{cases} R(s, a) + \gamma \cdot \mathbb{E}_{s' \sim P(\cdot | s, a)} V^\pi(s') & \text{if } s \neq s_{reset} \\ 0 & \text{otherwise; and} \end{cases} \\ 903 \\ 904 \\ 905 V^\pi(s) = \mathbb{E}_{a \sim \pi(\cdot | s)} Q^\pi(s, a). \\ 906$$

907 All our results extend to this formulation (cf. Remark 2).
 908

909 *Remark 1* (Occupancy measure). In RL theory, the discounted occupancy measure
 910

$$911 \mu_\pi^\gamma(s) := (1 - \gamma) \cdot \sum_{t=0}^{\infty} \gamma^t \mathbb{P}_\pi \left(\left\{ (s_i, a_i)_{i \geq 0} \mid s_t = s \right\} \right) \\ 912 \\ 913$$

914 is often considered as the default marginal distribution over states the agent visit along the interaction, mostly
 915 because of its suitable theoretical properties. In fact, for any arbitrary MDP, μ_π^γ is the **stationary distribution** of
 916 the episodic process obtained by considering a reset probability of $1 - \gamma$ from every state of the original MDP
 917 (Puterman, 1994; Metelli et al., 2023). Again, we contend that all our results can be extended to the occupancy
 918 measure with little effort.

918 **B POLICY IMPROVEMENTS THROUGH MIRROR LEARNING AND CONVERGENCE**
 919 **GUARANTEES**
 920

921 In this section, we prove that \mathcal{N}^C (Eq. 2) is a proper *mirror learning neighborhood operator*. As a consequence,
 922 appropriately updating the policy according to \mathcal{N}^C is guaranteed to be an instance of mirror learning, yielding the
 923 convergence guarantees of Theorem 1.

924 For completeness, we recall the definition of neighborhood operator from Kuba et al. (2022).

925 **Definition 1** (Neighborhood operator). *The mapping $\mathcal{N}: \Pi \rightarrow 2^\Pi$ is a (mirror learning) neighborhood operator, if*

926 *1. (continuity) It is a continuous map;*
 927 *2. (compactness) Every $\mathcal{N}(\pi)$ is a compact set; and*
 928 *3. (closed ball) There exists a metric $d: \Pi \times \Pi \rightarrow [0, \infty)$, such that for all policies $\pi \in \Pi$, there exists $\epsilon > 0$,
 929 *such that $d(\pi, \pi') \leq \epsilon$ implies $\pi' \in \mathcal{N}(\pi)$.**

930 The trivial neighborhood operator is $\mathcal{N}(\pi) = \Pi$.

931 **Lemma 1.** \mathcal{N}^C is a neighborhood operator.

932 *Proof.* Henceforth, fix a policy $\pi \in \Pi$. When taking the supremum, infimum, maximum, or minimum value
 933 over states and actions, we always consider actions to be taken from the support of the behavioral policy (in the
 934 denominator of the quotient).

935 Item 2 (compactness) is trivial due to $D_{\text{IR}}^{\text{inf}}(\pi, \pi') \geq 2 - C$ and $D_{\text{IR}}^{\text{sup}}(\pi, \pi') \leq C$ for any $\pi' \in \mathcal{N}^C(\pi)$. This
 936 means $\mathcal{N}^C(\pi)$ contains its extrema, i.e., all the policies π' satisfying $D_{\text{IR}}^{\text{inf}}(\pi, \pi') = 2 - C$ and $D_{\text{IR}}^{\text{sup}}(\pi, \pi') \leq C$,
 937 or $D_{\text{IR}}^{\text{inf}}(\pi, \pi') \geq 2 - C$ and $D_{\text{IR}}^{\text{sup}}(\pi, \pi') = C$.

938 In the following, for any $\pi \in \Pi$ and sequence $(\pi_n)_{n \geq 0}$, we write $\pi_n \rightarrow \pi$ for the convergence of the sequence to π
 939 with respect to the metric

$$d(\pi_1, \pi_2) = \begin{cases} \|\pi_1 - \pi_2\|_\infty & \text{if } \text{supp}(\pi_1(\cdot | s)) = \text{supp}(\pi_2(\cdot | s)) \quad \forall s \in \mathcal{S}, \text{ and} \\ 1 & \text{otherwise.} \end{cases} \quad (7)$$

940 In other words, $\pi_n \rightarrow \pi$ means that π_n converges to π in supremum norm as $n \rightarrow \infty$ when the support of the
 941 converging policy stabilizes and becomes the same as the limit policy.

942 Let us prove item 1 (continuity). We show that \mathcal{N}^C is a continuous *correspondence* by showing it is upper and
 943 lower *hemicontinuous* (Ok, 2007).

944 \mathcal{N}^C is *upper hemicontinuous* (uhc) if it is *compact-valued* (item 1) and, for all policies $\pi \in \Pi$ and every sequences
 945 $(\pi_n)_{n \geq 0}$ and $(\pi'_n)_{n \geq 0}$ with $\pi'_n \in \mathcal{N}^C(\pi_n)$ for all $n \geq 0$, $\pi_n \rightarrow \pi$ and $\pi'_n \rightarrow \pi'$ implies $\pi' \in \mathcal{N}^C(\pi)$. Let $(\pi_n)_{n \geq 0}$
 946 and $(\pi'_n)_{n \geq 0}$ be sequences of policies with $\pi'_n \in \mathcal{N}^C(\pi_n)$ for all $n \geq 0$.

947 Fix $s \in \mathcal{S}$ and $a \in \mathcal{A}$. Consider the mapping

$$f_{s,a}: \{(\pi, \pi') \in \Pi \times \Pi \mid a \in \text{supp}(\pi(\cdot | s))\} \rightarrow [0, \infty), \quad (\pi, \pi') \mapsto \frac{\pi'(a | s)}{\pi(a | s)}.$$

948 It is clear $f_{s,a}$ is continuous since the application of π to $\pi(a | s)$ is continuous and the division of two continuous
 949 functions is also continuous (when considering actions from the support of $\pi(\cdot | s)$). Importantly, for $\text{ext} \in \{\text{sup}, \text{inf}\}$,
 950 $D_{\text{IR}}^{\text{ext}}(\pi, \pi') = \text{ext} \{f_{s,a}(\pi, \pi'): s \in \mathcal{S}, a \in \text{supp}(\pi(\cdot | s))\}$ is also continuous: since \mathcal{S} and \mathcal{A} are
 951 finite, the supremum (resp. infimum) boils down to taking the maximum (resp. minimum) of finitely many many
 952 continuous functions, which is a continuous operation.

953 Now, assume that $\pi_n \rightarrow \pi$ and $\pi'_n \rightarrow \pi'$. The continuity of $D_{\text{IR}}^{\text{ext}}$ means that $D_{\text{IR}}^{\text{ext}}(\pi_n, \pi'_n) \rightarrow D_{\text{IR}}^{\text{ext}}(\pi, \pi')$. Since
 954 $\pi'_n \in \mathcal{N}^C(\pi_n)$, we have $D_{\text{IR}}^{\text{inf}}(\pi_n, \pi'_n) \geq 2 - C$ and $D_{\text{IR}}^{\text{sup}}(\pi_n, \pi'_n) \leq C$ for all $n \geq 0$. By the fact that $D_{\text{IR}}^{\text{ext}}(\pi_n, \pi'_n)$
 955 converges to $D_{\text{IR}}^{\text{ext}}(\pi, \pi')$ for $\text{ext} \in \{\text{inf}, \text{sup}\}$, we also have that $D_{\text{IR}}^{\text{inf}}(\pi, \pi') \geq 2 - C$ and $D_{\text{IR}}^{\text{sup}}(\pi, \pi') \leq C$.

956 Then, \mathcal{N}^C is uhc.

957 \mathcal{N}^C is *lower hemicontinuous* (lhc) if, for every policy π , sequence $(\pi_n)_{n \geq 0}$ with $\pi_n \rightarrow \pi$, and policy $\pi' \in \mathcal{N}^C(\pi)$,
 958 there exists a sequence $(\pi'_n)_{n \geq 0}$ with $\pi'_n \rightarrow \pi'$ and such that there is a $n_0 \geq 0$ from which, for all $n \geq n_0$,
 959 $\pi'_n \in \mathcal{N}^C(\pi_n)$. Therefore, let $(\pi_n)_{n \geq 0}$ be a sequence of policies so that $\pi_n \rightarrow \pi$ and $\pi' \in \mathcal{N}(\pi)$. Since $\pi_n \rightarrow \pi$,

972 we have

$$974 \quad \forall \delta > 0, \exists n_0 \in \mathbb{N}: \forall n \geq n_0, \|\pi_n - \pi\|_\infty \leq \delta \text{ and } \text{supp}(\pi_n(\cdot | s)) = \text{supp}(\pi(\cdot | s)) \quad \forall s \in \mathcal{S}.$$

975 In particular, this holds for $\delta < \pi_{\min}/2$, where $\pi_{\min} = \min \{\pi(a | s) : s \in \mathcal{S}, a \in \text{supp}(\pi(\cdot | s))\}$. Let $n_0 \geq 0$ be
976 the step associated with $\delta < \pi_{\min}/2$ and $n \geq n_0$. Write $\delta_n = \|\pi_n - \pi\|_\infty$ and let
977

$$978 \quad \epsilon_n = \frac{2C\delta_n}{\pi_{\min}(C-1) + 2C\delta_n} \in (0, 1)$$

980 Construct a sequence $(\pi'_n)_{n \geq 0}$ so that, for all $s \in \mathcal{S}$, $a \in \mathcal{A}$, and $n \geq n_0$,

$$982 \quad \pi'_n(a | s) = (1 - \epsilon_n) \cdot \pi'(a | s) + \epsilon_n \cdot \pi_n(a | s).$$

984 Intuitively, π'_n is a mixture of distributions $\pi'(\cdot | s)$ and $\pi_n(\cdot | s)$. Consequently, $\pi'_n(\cdot | s)$ is a well-defined
985 distribution. Finally, note that $\pi'_n \rightarrow \pi'$ because $\delta_n \rightarrow 0$, and so does ϵ_n .

986 Now, we restrict our attention to $a \in \text{supp}(\pi_n(\cdot | s))$. Note that since π_n stably converges to π with its support, π
987 has the same support as π_n . Furthermore, since $\pi' \in \mathcal{N}^C(C)$, π' has also the same support as π_n . In consequence,
988 π'_n has the same support as π_n .

989 Having that said, we start by showing the upper bound:

$$\begin{aligned} 991 \quad \frac{\pi'_n(a | s)}{\pi_n(a | s)} &= (1 - \epsilon_n) \frac{\pi'(a | s)}{\pi_n(a | s)} + \epsilon_n \\ 992 \quad &\leq (1 - \epsilon_n) \frac{C \cdot \pi(a | s)}{\pi_n(a | s)} + \epsilon_n && (\text{because } \pi'(a | s) \leq C \cdot \pi(a | s)) \\ 993 \quad &\leq (1 - \epsilon_n) \cdot \frac{C \cdot \pi(a | s)}{\pi(a | s) - \delta_n} + \epsilon_n && (\text{because } \pi_n(a | s) \geq \pi(a | s) - \delta_n) \\ 994 \quad &= (1 - \epsilon_n) \frac{C}{1 - \delta_n/\pi(a | s)} + \epsilon_n \\ 995 \quad &\leq (1 - \epsilon_n) \frac{C}{1 - \delta_n/\pi_{\min}} + \epsilon_n. \end{aligned}$$

1002 Note that for all $x \in [0, 1/2]$,

$$1004 \quad \frac{1}{1-x} \leq 1 + 2x \text{ because } 1 + 2x - \frac{1}{1-x} \geq 0 \iff \frac{(1+2x)(1-x)-1}{1-x} \geq 0 \iff \frac{x(1-2x)}{1-x} \geq 0.$$

1006 Then, since $0 < \delta_n/\pi_{\min} < 1/2$, we have

$$1008 \quad \frac{\pi'_n(a | s)}{\pi_n(a | s)} \leq (1 - \epsilon_n) \cdot C \cdot (1 + 2\delta_n/\pi_{\min}) + \epsilon_n.$$

1011 Let $x_n = 1 + \frac{2\delta_n}{\pi_{\min}}$, and note that

$$1013 \quad \epsilon_n = \frac{2C\delta_n}{\pi_{\min}(C-1) + 2C\delta_n} = \frac{2C \cdot \delta_n/\pi_{\min}}{C + 2C \cdot \delta_n/\pi_{\min} - 1} = \frac{-2C \cdot \delta_n/\pi_{\min}}{1 - C - 2C \cdot \delta_n/\pi_{\min}} = \frac{C(1 - x_n)}{1 - x_n \cdot C}.$$

1015 Then,

$$\begin{aligned} 1017 \quad \frac{\pi'_n(a | s)}{\pi_n(a | s)} &\leq (1 - \epsilon_n)x_n \cdot C + \epsilon_n \\ 1018 \quad &= x_n \cdot C - \epsilon_n \cdot x_n \cdot C + \epsilon_n \\ 1019 \quad &= x_n \cdot C - \frac{C(1 - x_n)}{1 - x_n \cdot C} \cdot x_n \cdot C + \frac{C(1 - x_n)}{1 - x_n \cdot C} \\ 1020 \quad &= \frac{x_n \cdot C(1 - x_n \cdot C) - x_n \cdot C^2(1 - x_n) + C(1 - x_n)}{1 - x_n \cdot C} \\ 1021 \quad &= \frac{x_n \cdot C - x_n^2 C^2 - x_n \cdot C^2 + x_n^2 C^2 + C - x_n \cdot C}{1 - x_n \cdot C} \end{aligned}$$

$$\begin{aligned}
1026 \quad &= \frac{-x_n \cdot C^2 + C}{1 - x_n \cdot C} \\
1027 \quad &= C \cdot \frac{1 - x_n \cdot C}{1 - x_n \cdot C} \\
1028 \quad &= C, \\
1029 \quad & \\
1030 \quad & \\
1031 \quad &
\end{aligned}$$

1032 which means that $D_{\text{IR}}^{\text{sup}}(\pi_n, \pi'_n) \leq C$.

1033 We now show the lower bound:

$$\begin{aligned}
1034 \quad \frac{\pi'_n(a | s)}{\pi_n(a | s)} &= (1 - \epsilon_n) \frac{\pi'(a | s)}{\pi_n(a | s)} + \epsilon_n \\
1035 \quad &\geq (1 - \epsilon_n) \frac{(2 - C) \cdot \pi(a | s)}{\pi_n(a | s)} + \epsilon_n && \text{(because } \pi'(a | s) \geq (2 - C) \cdot \pi(a | s)) \\
1036 \quad &\geq (1 - \epsilon_n) \frac{(2 - C) \cdot \pi(a | s)}{\pi(a | s) + \delta_n} + \epsilon_n && \text{(because } \pi_n(a | s) \leq \pi(a | s) + \delta_n) \\
1037 \quad &= (1 - \epsilon_n) \frac{(2 - C)}{1 + \delta_n / \pi(a | s)} + \epsilon_n \\
1038 \quad &\geq (1 - \epsilon_n) \frac{(2 - C)}{1 + \delta_n / \pi_{\min}} + \epsilon_n \\
1039 \quad &\geq (1 - \epsilon_n) \cdot (2 - C) \cdot (1 - \delta_n / \pi_{\min}) + \epsilon_n && \text{(because for all } x \in \mathbb{R}, \frac{1}{1+x} \geq 1 - x) \\
1040 \quad &= (1 - \epsilon_n) \cdot (2 - C - 2 \cdot \delta_n / \pi_{\min} + C \cdot \delta_n / \pi_{\min}) + \epsilon_n \\
1041 \quad &= (1 - \epsilon_n) \cdot (2 - C + (C - 2) \cdot \delta_n / \pi_{\min}) + \epsilon_n \\
1042 \quad &= 2 - C + (C - 2) \cdot \delta_n / \pi_{\min} - \epsilon_n (2 - C + (C - 2) \cdot \delta_n / \pi_{\min}) + \epsilon_n \\
1043 \quad &= 2 - C + (C - 2) \cdot \delta_n / \pi_{\min} + \epsilon_n (C - 1 + (2 - C) \cdot \delta_n / \pi_{\min}) \\
1044 \quad &= 2 - C + (C - 2) \cdot \delta_n / \pi_{\min} + \epsilon_n (C - 1) + \epsilon_n \cdot (2 - C) \cdot \delta_n / \pi_{\min} \\
1045 \quad &= 2 - C + (C - 2) \cdot \delta_n / \pi_{\min} + \frac{2C\delta_n \cdot (C - 1)}{\pi_{\min}(C - 1) + 2C\delta_n} + \frac{2C\delta_n \cdot (2 - C)}{\pi_{\min}(C - 1) + 2C\delta_n} \cdot \delta_n / \pi_{\min} \\
1046 \quad &= 2 - C + \delta_n \cdot \left(\frac{C - 2}{\pi_{\min}} + \frac{2C \cdot (C - 1)}{\pi_{\min}(C - 1) + 2C\delta_n} + \frac{2C\delta_n \cdot \pi_{\min}^{-1} \cdot (2 - C)}{\pi_{\min}(C - 1) + 2C\delta_n} \right) \\
1047 \quad &\geq 2 - C. \\
1048 \quad & \\
1049 \quad & \\
1050 \quad & \\
1051 \quad & \\
1052 \quad & \\
1053 \quad & \\
1054 \quad & \\
1055 \quad & \\
1056 \quad & \\
1057 \quad & \\
1058 \quad & \\
1059 \quad &
\end{aligned}$$

1060 To see how we obtain the last line, note that it suffices to show the content of the parenthesis multiplied by δ_n is
1061 greater than zero, i.e.,

$$\begin{aligned}
1062 \quad &\frac{C - 2}{\pi_{\min}} + \frac{2C \cdot (C - 1)}{\pi_{\min}(C - 1) + 2C\delta_n} + \frac{2C\delta_n \cdot \pi_{\min}^{-1} \cdot (2 - C)}{\pi_{\min}(C - 1) + 2C\delta_n} \geq 0 \\
1063 \quad &\iff \frac{2C \cdot (C - 1) + 2C\delta_n \cdot \pi_{\min}^{-1} \cdot (2 - C)}{\pi_{\min}(C - 1) + 2C\delta_n} \geq \frac{2 - C}{\pi_{\min}} \\
1064 \quad &\iff 2C\pi_{\min} \cdot (C - 1) + 2C\delta_n \cdot (2 - C) \geq (2 - C) \cdot (\pi_{\min}(C - 1) + 2C\delta_n) \\
1065 \quad &\iff 2C\pi_{\min} \cdot (C - 1) \geq (2 - C) \cdot (\pi_{\min}(C - 1) + 2C\delta_n - 2C\delta_n) \\
1066 \quad &\iff 2C\pi_{\min} \cdot (C - 1) \geq (2 - C) \cdot (\pi_{\min}(C - 1)) \\
1067 \quad &\iff 2C \geq 2 - C, \\
1068 \quad & \\
1069 \quad & \\
1070 \quad & \\
1071 \quad &
\end{aligned}$$

1072 which is always satisfied because $C \geq 1$. Therefore, since this holds for any $s \in \mathcal{S}$ and both π'_n and π_n have the
1073 same support, we have that $D_{\text{IR}}^{\text{inf}}(\pi, \pi') \geq 2 - C$.

1074 Thus, we have $D_{\text{IR}}^{\text{inf}}(\pi, \pi') \geq 2 - C$ and $D_{\text{IR}}^{\text{sup}}(\pi, \pi') \leq C$, $\pi'_n \in \mathcal{N}^C(\pi_n)$. Therefore, \mathcal{N}^C is lhc.
1075

1076 Since \mathcal{N}^C is uhc and lhc, it is continuous. This concludes the proof of item 1.

1077 It remains to show item 3. Let $\epsilon = (C - 1) \cdot \min_{s,a} \pi(a | s)$, with a taken from $\text{supp}(\pi(\cdot | s))$. Assume $d(\pi, \pi') \leq \epsilon$
1078 (cf. Eq. 7). For all $s \in \mathcal{S}, a \in \text{supp}(\pi(\cdot | s))$, we have
1079

$$\pi'(a | s)$$

$$\begin{aligned}
1080 &\leq \pi(a \mid s) + \epsilon \\
1081 &\leq \pi(a \mid s) + (C - 1) \cdot \min_{s,a} \pi(a \mid s) \\
1082 &\leq \pi(a \mid s) + (C - 1) \cdot \pi(a \mid s) \\
1083 &= \pi(a \mid s) \cdot (1 + C - 1) \\
1084 &= \pi(a \mid s) \cdot C, \\
1085 \\
1086
\end{aligned}$$

1087 or equivalently:

$$\begin{aligned}
1088 &\frac{\pi'(a \mid s)}{\pi(a \mid s)} \leq C. \\
1089
\end{aligned}$$

1090 It remains to show the lower bound:

$$\begin{aligned}
1091 &\pi'(a \mid s) \geq \pi(a \mid s) - \epsilon \\
1092 &= \pi(a \mid s) - (C - 1) \cdot \min_{s,a} \pi(a \mid s) \\
1093 &\geq \pi(a \mid s) - (C - 1) \cdot \pi(a \mid s) \\
1094 &= \pi(a \mid s) \cdot (1 - C + 1) \\
1095 &= \pi(a \mid s) \cdot C \\
1096 &\geq \pi(a \mid s)(2 - C), \\
1097 \\
1098
\end{aligned}$$

1099 or equivalently:

$$\begin{aligned}
1100 &\frac{\pi'(a \mid s)}{\pi(a \mid s)} \geq 2 - C. \\
1101 \\
1102
\end{aligned}$$

1103 This concludes the proof of item 3. \square

1104 Then, Theorem 1 is obtained as a corollary of Lemma 1, and the fact that the update process

$$\pi_{n+1} := \arg \sup_{\pi' \in \mathcal{N}^C(\pi_n)} \mathbb{E}_{s \sim \xi_{\pi_n}} \mathbb{E}_{a \sim \pi'(\cdot \mid s)} [A^{\pi_n}(s, a)],$$

1105 is an instance of mirror learning (Kuba et al., 2022).

1111 C CRUDE WASSERSTEIN UPPER BOUND

1112 **Lemma 2.** Let $s \in \mathcal{S}$ and $a \in \mathcal{A}$, the following upper bound holds:

$$\mathcal{W}(\phi_{\sharp} P(\cdot \mid s, a), \bar{P}(\cdot \mid \phi(s), a)) \leq \mathbb{E}_{s' \sim P(\cdot \mid s, a)} \mathbb{E}_{\bar{s}' \sim \bar{P}(\cdot \mid \phi(s), a)} \bar{d}(\phi(s'), \bar{s}').$$

1113 *Proof.*

$$\begin{aligned}
1114 &\mathcal{W}(\phi_{\sharp} P(\cdot \mid s, a), \bar{P}(\cdot \mid \phi(s), a)) \\
1115 &= \sup_{\|f\|_{\text{Lip}} \leq 1} \left[\mathbb{E}_{s' \sim P(\cdot \mid s, a)} f(\phi(s')) - \mathbb{E}_{\bar{s}' \sim \bar{P}(\cdot \mid \phi(s), a)} f(\bar{s}') \right] \\
1116 &\leq \mathbb{E}_{s' \sim P(\cdot \mid s, a)} \left[\sup_{\|f\|_{\text{Lip}} \leq 1} f(\phi(s')) - \mathbb{E}_{\bar{s}' \sim \bar{P}(\cdot \mid \phi(s), a)} f(\bar{s}') \right] \\
1117 &= \mathbb{E}_{s' \sim P(\cdot \mid s, a)} \mathcal{W}(\delta_{\phi(s')}, \bar{P}(\cdot \mid \phi(s), a)) \\
1118 &= \mathbb{E}_{s' \sim P(\cdot \mid s, a)} \left[\min_{\lambda \in \Lambda(\delta_{\phi(s')}, \bar{P}(\cdot \mid \phi(s), a))} \mathbb{E}_{(\bar{s}_1, \bar{s}_2) \sim \lambda} d(\bar{s}_1, \bar{s}_2) \right] \\
1119 &= \mathbb{E}_{s' \sim P(\cdot \mid s, a)} \mathbb{E}_{\bar{s}' \sim \bar{P}(\cdot \mid \phi(s), a)} \bar{d}(\phi(s'), \bar{s}'). \\
1120 \\
1121
\end{aligned} \tag{1}$$

1122 Here, (1) corresponds to the dual Kantorovich–Rubinstein formulation (Kantorovich and Rubinstein, 1958) where
1123 $\|\cdot\|_{\text{Lip}}$ corresponds to the Lipschitz norm, while (2) follows from the primal Monge formulation (Monge, 1781),
1124 with a trivial coupling induced by $\delta_{\phi(s')}$, the Dirac measure with impulse $\phi(s')$. \square

1134 **D REMARK ON SAFE POLICY IMPROVEMENT METHODS**
1135

1136 Standard principled *safe policy improvement* methods (SPI; Thomas et al., 2015; Ghavamzadeh et al., 2016a;
1137 Laroche et al., 2019; Simão et al., 2020; Castellini et al., 2023; Wienhöft et al., 2023) do not consider representation
1138 learning. Instead, SPI methods assume $\bar{\mathcal{S}} := \mathcal{S}$ and learn \bar{R} , \bar{P} by maximum likelihood estimation with respect to
1139 the experience stored in \mathcal{B} collected by the behavioral π_b . Then, the policy improvement relies on finding the best
1140 policy in $\bar{\mathcal{M}}$ that is (probably approximately correctly) guaranteed to improves on the behavioral policy (up to an
1141 error term $\zeta > 0$) against a set of all admissible MDPs, called *robust MDPs* (Iyengar, 2005; Nilim and Ghaoui,
1142 2005; Wiesemann et al., 2013; Ghavamzadeh et al., 2016b; Suilen et al., 2024):

$$1143 \quad \arg \sup_{\bar{\pi} \in \bar{\Pi}} \rho(\bar{\pi}, \bar{\mathcal{M}}) \quad \text{such that} \quad \arg \inf_{\mathcal{M}' \in \Xi(\bar{\mathcal{M}}, e)} \rho(\pi_b, \mathcal{M}') \geq \rho(\pi_b, \mathcal{M}') - \zeta, \text{ where} \\ 1144 \\ 1145 \\ 1146 \quad \Xi(\bar{\mathcal{M}}, e) := \left\{ \mathcal{M} = \langle \mathcal{S}, \mathcal{A}, P, R, s_I, \gamma \rangle \mid \begin{array}{l} |R(s, a) - \bar{R}(s, a)| \leq R_{\text{MAX}} \cdot e(s, a) \quad \text{and} \\ d_{\text{TV}}(P(\cdot \mid s, a), \bar{P}(\cdot \mid s, a)) \leq e(s, a) \quad \forall s \in \mathcal{S}, a \in \mathcal{A} \end{array} \right\}, \\ 1147 \\ 1148$$

1149 $e(s, a)$ being an *error* term depending on the number of times each state s and action a are present in the dataset \mathcal{B} ,
1150 and d_{TV} being the *total variation distance* (Müller, 1997) which boils down to the L_1 distance when the state-action
1151 space is finite. To provide *probably approximately correct* (PAC) guarantees, the state-action pairs need to be visited
1152 a *sufficient amount of time*, depending on the size of the state-action space, to ensure e is sufficiently small.
1153

1154 Note that the reward and total variation constraints are very related to our local losses L_R and L_P : the representation
1155 corresponds here to the identity and d_{TV} coincides with Wasserstein as the state space is discrete (Villani, 2009).
1156 The major difference here is that the bounds need to hold *globally*, i.e., for all state-action pairs, which make their
1157 computation typically intractable in complex settings (e.g., high-dimensional feature spaces).

1158 We argue **this objective is ill-suited to complex settings**. First, classic SPI does not apply to general spaces.
1159 Second, assuming we deal with *finite*, high-dimensional feature spaces (e.g., visual inputs or the RAM of a video
1160 game), it is simply unlikely that \mathcal{B} contains all state-action pairs. *SPI with baseline bootstrapping* (Laroche et al.,
1161 2019) allows bypassing this requirement by updating π_b only in state-action pairs where a *sufficient* number of
1162 samples are present in \mathcal{B} . Nevertheless, this number is gigantic and is linear in the state-action space while being
1163 exponential in the size of the encoding of γ and the desired error ζ . This deems the policy update intractable. Finally,
1164 as mentioned, standard SPI does not consider representation learning. This is a further obstacle to its application in
1165 complex settings.

1166 **E SAFE POLICY IMPROVEMENTS: PROOFS**
1167

1168 **Notations** Henceforth, we denote by $\bar{V}^{\bar{\pi}}$ the value function of the world model $\bar{\mathcal{M}}$ obtained under any latent policy
1169 $\bar{\pi} \in \bar{\Pi}$. When it is clear from the context that ϕ is the representation used jointly with a latent policy $\bar{\pi}$, we may
1170 simply write $\bar{V}^{\bar{\pi}}$ instead of $\bar{V}^{(\bar{\pi} \circ \phi)}$ for the value function of executing $\bar{\pi}$ in $\bar{\mathcal{M}}$. In the following, we may also write
1171 $(s, a) \sim \xi_{\pi}$ as a shorthand for first drawing $s \sim \xi_{\pi}$ and then $a \sim \pi(\cdot \mid s)$ for any policy $\pi \in \Pi$.
1172

1173 We start by recalling a result from Gelada et al. (2019) that will be useful in the subsequent proofs.
1174 **Lemma 3** (Lipschitzness of the *latent* value function). *Let $\bar{\mathcal{M}}$ be a latent MDP and $\bar{\pi}$ be a policy for $\bar{\mathcal{M}}$. Assume
1175 that $\bar{\mathcal{M}}$ has reward and transition constants $K_{\bar{R}}$ and $K_{\bar{P}}$ with $K_{\bar{P}}^{\bar{\pi}} < 1/\gamma$. Then, the latent value function is
1176 $K_{\bar{R}}^{\bar{\pi}}/(1-\gamma K_{\bar{P}}^{\bar{\pi}})$ -Lipschitz, i.e., for all $\bar{s}_1, \bar{s}_2 \in \bar{\mathcal{S}}$,*

$$1177 \\ 1178 \quad |\bar{V}^{\bar{\pi}}(\bar{s}_1) - \bar{V}^{\bar{\pi}}(\bar{s}_2)| \leq \frac{K_{\bar{R}}^{\bar{\pi}}}{1 - \gamma K_{\bar{P}}^{\bar{\pi}}} \cdot \bar{d}(\bar{s}_1, \bar{s}_2) \\ 1179$$

1180 Note that the bound is straightforward when the latent space is discrete and the discrete metric $\mathbb{1} \{\neq\}$ is chosen for
1181 \bar{d} : the largest possible difference in values is $2R_{\text{MAX}}/1-\gamma$.
1182

1183 We also consider bounding expected value difference between the original MDP and the latent MDP by the local
1184 losses evaluated with respect to a behavioral policy π_b . Importantly, the expectation is measured over states and
1185 actions generated according to π_b , whereas the values correspond to those evaluated under *another latent policy*
1186 $\bar{\pi}$. The following Lemma states that the value difference yielded by a latent policy can be measured according to
1187 another behavioral policy, provided that the latent policy lies within a well-defined neighborhood of the behavioral
1188 policy.

1188 **Lemma 4** (Average value difference bound). *Let $\pi_b \in \Pi$ be the behavioral policy, $(\bar{\pi} \circ \phi) \in \mathcal{N}^{1/\gamma}(\pi_b)$ so that
1189 $\bar{\pi} \in \bar{\Pi}$ and $\phi: \mathcal{S} \rightarrow \bar{\mathcal{S}}$ is a state representation. Assume $\bar{\mathcal{M}}$ is equipped by the Lipschitz constants $K_{\bar{R}}$ and $K_{\bar{P}}$ and
1190 let $K_V = K_{\bar{R}}/(1-\gamma K_{\bar{P}})$. Assume that $K_{\bar{P}}$ is strictly lower than $1/\gamma$. Then, the average difference of value of \mathcal{M} and
1191 $\bar{\mathcal{M}}$ under $\bar{\pi}$ is bounded by*

1193

$$1194 \mathbb{E}_{s \sim \xi_{\pi_b}} |V^{\bar{\pi}}(s) - \bar{V}^{\bar{\pi}}(\phi(s))| \leq \frac{L_R^{\xi_{\pi_b}} + \gamma K_V \cdot L_P^{\xi_{\pi_b}}}{1/D_{IR}^{\sup}(\pi_b, \bar{\pi}) - \gamma}.$$

1196

1197

1198 *Proof.* The proof follows by adapting the proof of (Gelada et al., 2019, Lemma 3) by taking extra care of the
1199 behavioral policy. Namely, we want to evaluate the value difference bound for the latent policy $\bar{\pi}$, assuming states
1200 and actions are/have been produced by executing the behavioral policy π_b . The idea is to incorporate the divergence
1201 from π_b to $\bar{\pi}$ in the bound, formalized as the supremum IR between the underlying distribution of the two policies.

1202

$$1203 \mathbb{E}_{s \sim \xi_{\pi_b}} |V^{\bar{\pi}}(s) - \bar{V}^{\bar{\pi}}(\phi(s))|$$

1204

$$1205 = \mathbb{E}_{s \sim \xi_{\pi_b}} \left| a \sim \bar{\pi}(\cdot | \phi(s)) \left[R(s, a) + \gamma \mathbb{E}_{s' \sim P(\cdot | s, a)} [V^{\bar{\pi}}(s')] \right] - \mathbb{E}_{a \sim \bar{\pi}(\cdot | \phi(s))} \left[\bar{R}(\phi(s), a) + \gamma \mathbb{E}_{\bar{s}' \sim \bar{P}(\cdot | \phi(s), a)} [\bar{V}^{\bar{\pi}}(\bar{s}')] \right] \right|$$

1206

$$1207 = \mathbb{E}_{s \sim \xi_{\pi_b}} \left| a \sim \bar{\pi}(\cdot | \phi(s)) \left[R(s, a) - \bar{R}(\phi(s), a) \right] + \gamma \mathbb{E}_{a \sim \bar{\pi}(\cdot | \phi(s))} \left[\mathbb{E}_{\substack{s' \sim P(\cdot | s, a) \\ \bar{s}' \sim \bar{P}(\cdot | \phi(s), a)}} [V^{\bar{\pi}}(s') - \bar{V}^{\bar{\pi}}(\bar{s}')] \right] \right|$$

1208

$$1209 = \mathbb{E}_{s \sim \xi_{\pi_b}} \left| a \sim \bar{\pi}(\cdot | \phi(s)) \left[R(s, a) - \bar{R}(\phi(s), a) \right] + \gamma \mathbb{E}_{a \sim \bar{\pi}(\cdot | \phi(s))} \left[\mathbb{E}_{\substack{s' \sim P(\cdot | s, a) \\ \bar{s}' \sim \bar{P}(\cdot | \phi(s), a)}} [V^{\bar{\pi}}(s') - \bar{V}^{\bar{\pi}}(\phi(s')) + \bar{V}^{\bar{\pi}}(\phi(s')) - \bar{V}^{\bar{\pi}}(\bar{s}')] \right] \right|$$

1210

$$1211 = \mathbb{E}_{s \sim \xi_{\pi_b}} \left| a \sim \bar{\pi}(\cdot | \phi(s)) \left[R(s, a) - \bar{R}(\phi(s), a) \right] \right. \\ 1212 \left. + \gamma \mathbb{E}_{a \sim \bar{\pi}(\cdot | \phi(s))} \left[\mathbb{E}_{\substack{s' \sim P(\cdot | s, a) \\ \bar{s}' \sim \bar{P}(\cdot | \phi(s), a)}} [V^{\bar{\pi}}(s') - \bar{V}^{\bar{\pi}}(\phi(s'))] + \mathbb{E}_{\substack{s' \sim P(\cdot | s, a) \\ \bar{s}' \sim \bar{P}(\cdot | \phi(s), a)}} [\bar{V}^{\bar{\pi}}(\phi(s')) - \bar{V}^{\bar{\pi}}(\bar{s}')] \right] \right|$$

1213

$$1214 \leq \mathbb{E}_{s \sim \xi_{\pi_b}} \mathbb{E}_{a \sim \bar{\pi}(\cdot | \phi(s))} \left| \left[R(s, a) - \bar{R}(\phi(s), a) \right] + \gamma \mathbb{E}_{s' \sim P(\cdot | s, a)} [V^{\bar{\pi}}(s') - \bar{V}^{\bar{\pi}}(\phi(s'))] + \gamma \mathbb{E}_{\substack{s' \sim P(\cdot | s, a) \\ \bar{s}' \sim \bar{P}(\cdot | \phi(s), a)}} [\bar{V}^{\bar{\pi}}(\phi(s')) - \bar{V}^{\bar{\pi}}(\bar{s}')] \right| \\ 1215 \quad \quad \quad \text{(Jensen's inequality)}$$

1216

$$1217 \leq \mathbb{E}_{s \sim \xi_{\pi_b}} \mathbb{E}_{a \sim \bar{\pi}(\cdot | \phi(s))} |R(s, a) - \bar{R}(\phi(s), a)| + \gamma \mathbb{E}_{s \sim \xi_{\pi_b}} \mathbb{E}_{a \sim \bar{\pi}(\cdot | \phi(s))} \left| \mathbb{E}_{\substack{s' \sim P(\cdot | s, a) \\ \bar{s}' \sim \bar{P}(\cdot | \phi(s), a)}} [\bar{V}^{\bar{\pi}}(\phi(s')) - \bar{V}^{\bar{\pi}}(\bar{s}')] \right| \\ 1218 \quad \quad \quad + \gamma \mathbb{E}_{s \sim \xi_{\pi_b}} \mathbb{E}_{a \sim \bar{\pi}(\cdot | \phi(s))} \left| \mathbb{E}_{\substack{s' \sim P(\cdot | s, a) \\ \bar{s}' \sim \bar{P}(\cdot | \phi(s), a)}} [V^{\bar{\pi}}(s') - \bar{V}^{\bar{\pi}}(\phi(s'))] \right| \\ 1219 \quad \quad \quad \text{(Triangle inequality)}$$

1220

$$1221 = \mathbb{E}_{s \sim \xi_{\pi_b}} \mathbb{E}_{a \sim \pi_b(\cdot | s)} \left| \frac{\bar{\pi}(a | \phi(s))}{\pi_b(a | s)} \mathbb{E}_{\substack{s' \sim P(\cdot | s, a) \\ \bar{s}' \sim \bar{P}(\cdot | \phi(s), a)}} [\bar{V}^{\bar{\pi}}(\phi(s')) - \bar{V}^{\bar{\pi}}(\bar{s}')] \right| \\ 1222 \quad \quad \quad + \gamma \mathbb{E}_{s \sim \xi_{\pi_b}} \mathbb{E}_{a \sim \pi_b(\cdot | s)} \left| \frac{\bar{\pi}(a | \phi(s))}{\pi_b(a | s)} \mathbb{E}_{\substack{s' \sim P(\cdot | s, a) \\ \bar{s}' \sim \bar{P}(\cdot | \phi(s), a)}} [V^{\bar{\pi}}(s') - \bar{V}^{\bar{\pi}}(\phi(s'))] \right| \\ 1223 \quad \quad \quad \text{(because } \text{supp}(\bar{\pi}(\cdot | \phi(s))) = \text{supp}(\pi_b(\cdot | s)) \text{ for all } s \in \mathcal{S})$$

$$\begin{aligned}
& \leq D_{\text{IR}}^{\sup}(\pi_b, \bar{\pi}) \mathbb{E}_{s, a \sim \xi_{\pi_b}} |R(s, a) - \bar{R}(\phi(s), a)| + \gamma \cdot D_{\text{IR}}^{\sup}(\pi_b, \bar{\pi}) \mathbb{E}_{s, a \sim \xi_{\pi_b}} \left| \mathbb{E}_{\bar{s}' \sim \phi_{\sharp} P(\cdot | s, a)} \bar{V}^{\bar{\pi}}(\bar{s}') - \mathbb{E}_{\bar{s}' \sim \bar{P}(\cdot | \phi(s), a)} \bar{V}^{\bar{\pi}}(\bar{s}') \right| \\
& \quad + \gamma \cdot D_{\text{IR}}^{\sup}(\pi_b, \bar{\pi}) \mathbb{E}_{s, a \sim \xi_{\pi_b}} \left| \mathbb{E}_{s' \sim P(\cdot | s, a)} [V^{\bar{\pi}}(s') - \bar{V}^{\bar{\pi}}(\phi(s'))] \right| \\
& \quad (\text{because } D_{\text{IR}}^{\sup}(\pi_b, \bar{\pi}) = \sup_{s, a} \left[\frac{\bar{\pi}(a | \phi(s))}{\pi_b(\cdot | s)} \right]) \\
& = D_{\text{IR}}^{\sup}(\pi_b, \bar{\pi}) \cdot L_R^{\xi_{\pi_b}} + \gamma \cdot D_{\text{IR}}^{\sup}(\pi_b, \bar{\pi}) \mathbb{E}_{s, a \sim \xi_{\pi_b}} \left| \mathbb{E}_{\bar{s}' \sim \phi_{\sharp} P(\cdot | s, a)} \bar{V}^{\bar{\pi}}(\bar{s}') - \mathbb{E}_{\bar{s}' \sim \bar{P}(\cdot | \phi(s), a)} \bar{V}^{\bar{\pi}}(\bar{s}') \right| \\
& \quad + \gamma \cdot D_{\text{IR}}^{\sup}(\pi_b, \bar{\pi}) \mathbb{E}_{s, a \sim \xi_{\pi_b}} \left| \mathbb{E}_{s' \sim P(\cdot | s, a)} [V^{\bar{\pi}}(s') - \bar{V}^{\bar{\pi}}(\phi(s'))] \right| \\
& \quad (\text{by definition of } L_R^{\xi_{\pi_b}}) \\
& \leq D_{\text{IR}}^{\sup}(\pi_b, \bar{\pi}) \cdot L_R^{\xi_{\pi_b}} + \gamma K_V \cdot D_{\text{IR}}^{\sup}(\pi_b, \bar{\pi}) \mathbb{E}_{s, a \sim \xi_{\pi_b}} \mathcal{W}_{\bar{d}}(\phi_{\sharp} P(\cdot | s, a), \bar{P}(\cdot | \phi(s), a)) \\
& \quad + \gamma \cdot D_{\text{IR}}^{\sup}(\pi_b, \bar{\pi}) \mathbb{E}_{s, a \sim \xi_{\pi_b}} \left| \mathbb{E}_{s' \sim P(\cdot | s, a)} [V^{\bar{\pi}}(s') - \bar{V}^{\bar{\pi}}(\phi(s'))] \right| \\
& \quad (\text{by Theorem 3 and the dual formulation of Wasserstein}) \\
& = D_{\text{IR}}^{\sup}(\pi_b, \bar{\pi}) \cdot (L_R^{\xi_{\pi_b}} + \gamma K_V \cdot L_P^{\xi_{\pi_b}}) + \gamma D_{\text{IR}}^{\sup}(\pi_b, \bar{\pi}) \cdot \mathbb{E}_{s, a \sim \xi_{\pi_b}} \left| \mathbb{E}_{s' \sim P(\cdot | s, a)} [V^{\bar{\pi}}(s') - \bar{V}^{\bar{\pi}}(\phi(s'))] \right| \\
& \quad (\text{by definition of } L_P^{\xi_{\pi_b}}) \\
& \leq D_{\text{IR}}^{\sup}(\pi_b, \bar{\pi}) \cdot (L_R^{\xi_{\pi_b}} + \gamma K_V \cdot L_P^{\xi_{\pi_b}}) + \gamma D_{\text{IR}}^{\sup}(\pi_b, \bar{\pi}) \cdot \mathbb{E}_{s, a \sim \xi_{\pi_b}} \mathbb{E}_{s' \sim P(\cdot | s, a)} |V^{\bar{\pi}}(s') - \bar{V}^{\bar{\pi}}(\phi(s'))| \\
& \quad (\text{Jensen's inequality}) \\
& = D_{\text{IR}}^{\sup}(\pi_b, \bar{\pi}) \cdot (L_R^{\xi_{\pi_b}} + \gamma K_V \cdot L_P^{\xi_{\pi_b}}) + \gamma D_{\text{IR}}^{\sup}(\pi_b, \bar{\pi}) \cdot \mathbb{E}_{s \sim \xi_{\pi_b}} |V^{\bar{\pi}}(s) - \bar{V}^{\bar{\pi}}(\phi(s))| \\
& \quad (\text{as } \xi_{\pi_b} \text{ is a stationary measure})
\end{aligned}$$

1272 To summarize, we have:

$$1273 \mathbb{E}_{s \sim \xi_{\pi_b}} |V^{\bar{\pi}}(s) - \bar{V}^{\bar{\pi}}(\phi(s))| \leq D_{\text{IR}}^{\sup}(\pi_b, \bar{\pi}) \cdot (L_R^{\xi_{\pi_b}} + \gamma K_V \cdot L_P^{\xi_{\pi_b}}) + \gamma D_{\text{IR}}^{\sup}(\pi_b, \bar{\pi}) \cdot \mathbb{E}_{s \sim \xi_{\pi_b}} |V^{\bar{\pi}}(s) - \bar{V}^{\bar{\pi}}(\phi(s))|.$$

1276 Or equivalently,

$$\begin{aligned}
1277 (1 - \gamma D_{\text{IR}}^{\sup}(\pi_b, \bar{\pi})) \mathbb{E}_{s \sim \xi_{\pi_b}} |V^{\bar{\pi}}(s) - \bar{V}^{\bar{\pi}}(\phi(s))| & \leq D_{\text{IR}}^{\sup}(\pi_b, \bar{\pi}) \cdot (L_R^{\xi_{\pi_b}} + \gamma K_V \cdot L_P^{\xi_{\pi_b}}) \\
1280 \mathbb{E}_{s \sim \xi_{\pi_b}} |V^{\bar{\pi}}(s) - \bar{V}^{\bar{\pi}}(\phi(s))| & \leq D_{\text{IR}}^{\sup}(\pi_b, \bar{\pi}) \cdot \frac{L_R^{\xi_{\pi_b}} + \gamma K_V \cdot L_P^{\xi_{\pi_b}}}{1 - \gamma D_{\text{IR}}^{\sup}(\pi_b, \bar{\pi})} \\
1283 & = \frac{L_R^{\xi_{\pi_b}} + \gamma K_V \cdot L_P^{\xi_{\pi_b}}}{1/D_{\text{IR}}^{\sup}(\pi_b, \bar{\pi}) - \gamma},
\end{aligned}$$

1285 which is well-defined because $D_{\text{IR}}^{\sup}(\pi_b, \bar{\pi})$ is assumed strictly lower than $1/\gamma$. \square

1287

1288 In the main text, we made the assumption the environment is episodic. Let us formally restate this assumption:

1289 **Assumption 2.** *The environment \mathcal{M} and the world model $\bar{\mathcal{M}}$ are episodic.*

1290 **Assumption 3.** $\forall s \in \mathcal{S}, \phi(s) = \bar{s}_{\text{reset}}$ if and only if $s = s_{\text{reset}}$.

1291 Note that, as mentioned in Section 2, Assumption 2 ensures the existence of a stationary distribution ξ_{π} and the
1292 ergodicity of both the original environment and the latent model. Assumption 3 guarantees that the reset states are
1293 aligned in the original and latent MDPs.

1294 We are now ready to prove Theorem 2.
1295

1296 **Theorem 2.** Suppose $\gamma > 1/2$ and $K_{\bar{P}}^{\bar{\pi}} < 1/\gamma$. Let $C \in (1, 1/\gamma)$, $\pi_b \in \Pi$ be the base policy, $(\bar{\pi} \circ \phi) \in \mathcal{N}^C(\pi_b)$
 1297 where $\bar{\pi} \in \bar{\Pi}$ is a latent policy and $\phi: \mathcal{S} \rightarrow \bar{\mathcal{S}}$ a state representation. Then,
 1298

$$1299 \quad 1300 \quad 1301 \quad |\rho(\bar{\pi} \circ \phi, \mathcal{M}) - \rho(\bar{\pi}, \bar{\mathcal{M}})| \leq \text{AEL}(\pi_b) \cdot \frac{L_R^{\xi_{\pi_b}}/\gamma + K_V \cdot L_P^{\xi_{\pi_b}}}{1/D_{IR}^{\text{sup}}(\pi_b, \bar{\pi}) - \gamma},$$

1302 where $\text{AEL}(\pi_b)$ denotes the average episode length when \mathcal{M} runs under π_b , $K_V = K_{\bar{R}}^{\bar{\pi}} / (1 - \gamma K_{\bar{P}}^{\bar{\pi}})$, and $L_R^{\xi_{\pi_b}}, L_P^{\xi_{\pi_b}}$
 1303 are the local losses of Eq. 4 over the stationary distribution ξ_{π_b} induced by π_b .
 1304

1305 *Proof.* The first part of the proof follows by the expected value difference bound of Lemma 4. The second part
 1306 of the proof follows by adapting of the one of Delgrange et al., 2025, Theorem 1, where the authors considered
 1307 discrete latent MDPs and reach-avoid objectives (rewards were disregarded).
 1308

1309 Our goal is to get rid of the expectation. First, note that for any measurable state so that $\xi_{\pi_b}(\{s\}) > 0$, we have
 1310 $|V^{\bar{\pi}}(s) - \bar{V}^{\bar{\pi}}(\phi(s))| \leq 1/\xi_{\pi_b}(\{s\}) \cdot \mathbb{E}_{s' \sim \xi_{\pi_b}} |V^{\bar{\pi}}(s') - \bar{V}^{\bar{\pi}}(\phi(s'))|$. For simplicity, we write $\xi_{\pi_b}(s)$ as shorthand
 1311 for $\xi_{\pi_b}(\{s\})$ when considering such states. Second, note that as s_{reset} is almost surely visited episodically (Assump-
 1312 tion 2), restarting the MDP (i.e., visiting s_{reset}) is a measurable event, meaning that s_{reset} has a non-zero probability
 1313 $\xi_{\pi_b}(s_{\text{reset}}) \in (0, 1)$. Then,

$$1314 \quad 1315 \quad |\rho(\bar{\pi} \circ \phi, \mathcal{M}) - \rho(\bar{\pi}, \bar{\mathcal{M}})| \quad (8)$$

$$1316 \quad = |V^{\bar{\pi}}(s_I) - \bar{V}^{\bar{\pi}}(\bar{s}_I)| \quad (9)$$

$$1317 \quad = \frac{1}{\gamma} |\gamma \cdot V^{\bar{\pi}}(s_I) - \gamma \cdot \bar{V}^{\bar{\pi}}(\bar{s}_I)| \quad (10)$$

$$1319 \quad = \frac{1}{\gamma} |V^{\bar{\pi}}(s_{\text{reset}}) - \bar{V}^{\bar{\pi}}(\phi(s_{\text{reset}}))| \quad (\text{by Assumptions 2 and 3})$$

$$1322 \quad \leq \frac{1}{\gamma \cdot \xi_{\pi_b}(s_{\text{reset}})} \mathbb{E}_{s \sim \xi_{\pi_b}} |V^{\bar{\pi}}(s) - \bar{V}^{\bar{\pi}}(\phi(s))| \quad (11)$$

$$1324 \quad \leq \frac{L_R^{\xi_{\pi_b}}/\gamma + K_V \cdot L_P^{\xi_{\pi_b}}}{\xi_{\pi_b}(s_{\text{reset}})(1/D_{IR}^{\text{sup}}(\pi_b, \bar{\pi}) - \gamma)}. \quad (12)$$

1327 Finally, the result follows from the fact that $1/\xi_{\pi_b}(s_{\text{reset}})$ corresponds to the AEL. Indeed, when \mathcal{M} is episodic, it is
 1328 irreducible and recurrent (Huang, 2020); thus, given the random variable

$$1329 \quad 1330 \quad \mathbf{T}_s(\tau = s_0, a_0, s_1, a_1, \dots) = \sum_{T=1}^{\infty} T \cdot \mathbb{1} \{s_T = s \text{ and } s_t \neq s \text{ for all } 0 < t < T\},$$

1332 we have $\xi_{\pi}(s) = 1/\mathbb{E}_{\pi}[\mathbf{T}_s | s_0 = s]$ for any $s \in \mathcal{S}$ and stationary policy π , where $\mathbb{E}_{\pi}[\mathbf{T}_s | s_0 = s]$ is the *mean*
 1333 *recurrence time* of s under π (Serfoso, 2009, Chapter 1, Theorem 54). In particular, this means that $1/\xi_{\pi_b}(s_{\text{reset}}) =$
 1334 $\mathbb{E}_{\pi_b}[\mathbf{T}_{s_{\text{reset}}} | s_0 = s_{\text{reset}}] = \mathbb{E}_{\pi_b}[\mathbf{T}]$ is the AEL of \mathcal{M} under π_b , which yields
 1335

$$1336 \quad 1337 \quad 1338 \quad |\rho(\bar{\pi} \circ \phi, \mathcal{M}) - \rho(\bar{\pi}, \bar{\mathcal{M}})| \leq \mathbb{E}_{\pi_b}[\mathbf{T}] \cdot \frac{L_R^{\xi_{\pi_b}}/\gamma + K_V \cdot L_P^{\xi_{\pi_b}}}{1/D_{IR}^{\text{sup}}(\pi_b, \bar{\pi}) - \gamma}.$$

□

1343 *Remark 2* (Extension to episodic value functions). In Lemma 4 and Theorem 2, we considered the standard
 1344 definition of value function. One may wonder whether the results hold when considering episodic value functions,
 1345 as defined in Appendix A. It turns out that it is the case, as one can easily adapt the proofs for those particular value
 1346 functions.

1347 We start by adapting the proof of Lemma 4:

$$1349 \quad \mathbb{E}_{s \sim \xi_{\pi_b}} |V^{\bar{\pi}}(s) - \bar{V}^{\bar{\pi}}(\phi(s))|$$

$$\begin{aligned}
&= \mathbb{E}_{s \sim \xi_{\pi_b}} \left| \mathbb{1}_{\{s \neq s_{reset}\}} \cdot \left(\begin{aligned} &\mathbb{E}_{a \sim \bar{\pi}(\cdot | \phi(s))} \left[R(s, a) + \gamma \mathbb{E}_{s' \sim P(\cdot | s, a)} [V^{\bar{\pi}}(s')] \right] \\ &- \mathbb{E}_{a \sim \bar{\pi}(\cdot | \phi(s))} \left[\bar{R}(\phi(s), a) + \gamma \mathbb{E}_{\bar{s}' \sim \bar{P}(\cdot | \phi(s), a)} [\bar{V}^{\bar{\pi}}(\bar{s}')] \right] \end{aligned} \right) \right| \\
&\leq \mathbb{E}_{s \sim \xi_{\pi_b}} \left| \mathbb{E}_{a \sim \bar{\pi}(\cdot | \phi(s))} \left[R(s, a) + \gamma \mathbb{E}_{s' \sim P(\cdot | s, a)} [V^{\bar{\pi}}(s')] \right] - \mathbb{E}_{a \sim \bar{\pi}(\cdot | \phi(s))} \left[\bar{R}(\phi(s), a) + \gamma \mathbb{E}_{\bar{s}' \sim \bar{P}(\cdot | \phi(s), a)} [\bar{V}^{\bar{\pi}}(\bar{s}')] \right] \right|.
\end{aligned}$$

1359 The remaining of the proof is identical.

1360 Concerning Theorem 2, we take a detour by defining a new value function U as

$$\begin{aligned}
1362 \quad U^{\bar{\pi}}(s) &= \mathbb{E}_{a \sim \bar{\pi}(\cdot | \phi(s))} \left[R(s, a) + \gamma \cdot \mathbb{E}_{s' \sim P(\cdot | s, a)} [U^{\bar{\pi}}(s') \cdot \mathbb{1}_{\{s' \neq s_{reset}\}}] \right] \quad \forall s \in \mathcal{S}
\end{aligned}$$

1364 The latent counterpart $\bar{U}^{\bar{\pi}}$ is defined similarly. By definition of the episodic value function (Appendix A) and since
1365 $V^{\bar{\pi}}(s_{reset}) = 0$, it is clear that
1366

$$\begin{aligned}
1367 \quad V^{\bar{\pi}}(s) &= \begin{cases} U^{\bar{\pi}}(s) & \text{if } s \neq s_{reset} \\ U^{\bar{\pi}}(s) \cdot \mathbb{1}_{\{s \neq s_{reset}\}} & \text{otherwise; and} \end{cases} \quad \bar{V}^{\bar{\pi}}(\bar{s}) = \begin{cases} \bar{U}^{\bar{\pi}}(\bar{s}) & \text{if } \bar{s} \neq \phi(s_{reset}) \\ \bar{U}^{\bar{\pi}}(\bar{s}) \cdot \mathbb{1}_{\{\bar{s} \neq \phi(s_{reset})\}} & \text{otherwise.} \end{cases} \quad (13)
\end{aligned}$$

1371 Therefore,

$$\begin{aligned}
1372 \quad &\mathbb{E}_{s \sim \xi_{\pi_b}} |U^{\bar{\pi}}(s) - \bar{U}^{\bar{\pi}}(\phi(s))| \\
1373 \quad &\leq \mathbb{E}_{s, a \sim \xi_{\pi_b}} \left[\frac{\bar{\pi}(a | \phi(s))}{\pi_b(a | s)} \cdot |R(s, a) - \bar{R}(\phi(s), a)| \right] \\
1374 \quad &\quad + \gamma \mathbb{E}_{s, a \sim \xi_{\pi_b}} \left[\frac{\bar{\pi}(a | \phi(s))}{\pi_b(a | s)} \cdot \left| \mathbb{E}_{s' \sim P(\cdot | s, a)} [U^{\bar{\pi}}(s') \cdot \mathbb{1}_{\{s' \neq s_{reset}\}}] - \mathbb{E}_{\bar{s}' \sim \bar{P}(\phi(s), a)} [\bar{U}^{\bar{\pi}}(\bar{s}') \cdot \mathbb{1}_{\{\bar{s}' \neq \phi(s_{reset})\}}] \right| \right] \\
1375 \quad &\quad \text{(Triangle inequality and importance sampling)} \\
1376 \quad &= D_{\text{IR}}^{\text{sup}}(\pi_b, \bar{\pi}) \cdot \mathbb{E}_{s, a \sim \xi_{\pi_b}} |R(s, a) - \bar{R}(\phi(s), a)| + \gamma D_{\text{IR}}^{\text{sup}}(\pi_b, \bar{\pi}) \cdot \mathbb{E}_{s, a \sim \xi_{\pi_b}} \left| \mathbb{E}_{s' \sim P(\cdot | s, a)} V^{\bar{\pi}}(s') - \mathbb{E}_{\bar{s}' \sim \bar{P}(\cdot | \phi(s), a)} \bar{V}^{\bar{\pi}}(\bar{s}') \right| \\
1377 \quad &\quad \text{(by Eq. 13 and definition of the SIR)}
\end{aligned}$$

$$\begin{aligned}
1378 \quad &\leq D_{\text{IR}}^{\text{sup}}(\pi_b, \bar{\pi}) \cdot \mathbb{E}_{s, a \sim \xi_{\pi_b}} |R(s, a) - \bar{R}(\phi(s), a)| + \gamma \cdot D_{\text{IR}}^{\text{sup}}(\pi_b, \bar{\pi}) \cdot \mathbb{E}_{s, a \sim \xi_{\pi_b}} \left| \mathbb{E}_{s' \sim P(\cdot | s, a)} [V^{\bar{\pi}}(s') - \bar{V}^{\bar{\pi}}(\phi(s'))] \right| \\
1379 \quad &\quad + \gamma \cdot D_{\text{IR}}^{\text{sup}}(\pi_b, \bar{\pi}) \cdot \mathbb{E}_{s, a \sim \xi_{\pi_b}} \left| \mathbb{E}_{\bar{s}' \sim \phi_{\sharp} P(\cdot | s, a)} \bar{V}^{\bar{\pi}}(\bar{s}') - \mathbb{E}_{\bar{s}' \sim \bar{P}(\cdot | \phi(s), a)} \bar{V}^{\bar{\pi}}(\bar{s}') \right| \\
1380 \quad &\quad \text{(Triangle inequality)}
\end{aligned}$$

$$\begin{aligned}
1381 \quad &\leq D_{\text{IR}}^{\text{sup}}(\pi_b, \bar{\pi}) \cdot L_R^{\xi_{\pi_b}} + \gamma D_{\text{IR}}^{\text{sup}}(\pi_b, \bar{\pi}) \cdot \mathbb{E}_{s \sim \xi_{\pi_b}} |V^{\bar{\pi}}(s) - \bar{V}^{\bar{\pi}}(\phi(s))| + \gamma D_{\text{IR}}^{\text{sup}}(\pi_b, \bar{\pi}) \cdot K_V \cdot L_P^{\xi_{\bar{\pi}}} \\
1382 \quad &\quad \text{(by the same developments as in the proof of Lemma 4)}
\end{aligned}$$

$$\begin{aligned}
1383 \quad &\leq D_{\text{IR}}^{\text{sup}}(\pi_b, \bar{\pi}) \cdot L_R^{\xi_{\bar{\pi}}} + \gamma D_{\text{IR}}^{\text{sup}}(\pi_b, \bar{\pi}) \cdot \frac{L_R^{\xi_{\pi_b}} + \gamma K_V \cdot L_P^{\xi_{\pi_b}}}{1/D_{\text{IR}}^{\text{sup}}(\pi_b, \bar{\pi}) - \gamma} + \gamma D_{\text{IR}}^{\text{sup}}(\pi_b, \bar{\pi}) \cdot K_V \cdot L_P^{\xi_{\bar{\pi}}} \quad (\text{Lemma 4})
\end{aligned}$$

$$\begin{aligned}
1384 \quad &= D_{\text{IR}}^{\text{sup}}(\pi_b, \bar{\pi}) \left(L_R^{\xi_{\pi_b}} \left(1 + \frac{\gamma}{D_{\text{IR}}^{\text{sup}}(\pi_b, \bar{\pi})^{-1} - \gamma} \right) + \gamma K_V \cdot L_P^{\xi_{\pi_b}} \left(1 + \frac{\gamma}{D_{\text{IR}}^{\text{sup}}(\pi_b, \bar{\pi})^{-1} - \gamma} \right) \right)
\end{aligned}$$

$$\begin{aligned}
1385 \quad &= D_{\text{IR}}^{\text{sup}}(\pi_b, \bar{\pi}) \left(L_R^{\xi_{\pi_b}} \cdot \gamma K_V \cdot L_P^{\xi_{\pi_b}} \right) \left(1 + \frac{\gamma}{D_{\text{IR}}^{\text{sup}}(\pi_b, \bar{\pi})^{-1} - \gamma} \right)
\end{aligned}$$

$$\begin{aligned}
1386 \quad &= \frac{L_R^{\xi_{\pi_b}} + \gamma K_V \cdot L_P^{\xi_{\pi_b}}}{1/D_{\text{IR}}^{\text{sup}}(\pi_b, \bar{\pi}) - \gamma}.
\end{aligned}$$

1404 Now, in the proof of Theorem 2, it suffices to replace Equation 9 by observing that, in the episodic case, we have
1405

$$1406 \quad |\rho(\bar{\pi} \circ \phi, \mathcal{M}) - \rho(\bar{\pi}, \bar{\mathcal{M}})| = |V^{\bar{\pi}}(s_I) - \bar{V}^{\bar{\pi}}(\bar{s}_I)| = |U^{\bar{\pi}}(s_I) - \bar{U}^{\bar{\pi}}(\bar{s}_I)| \quad (\text{again, by Equation 13})$$

$$1407 \quad = \frac{1}{\gamma} |\gamma \cdot U^{\bar{\pi}}(s_I) - \gamma \cdot \bar{U}^{\bar{\pi}}(\bar{s}_I)| = \frac{1}{\gamma} |U^{\bar{\pi}}(s_{\text{reset}}) - \bar{U}^{\bar{\pi}}(\phi(s_{\text{reset}}))|$$

1409 Modulo this change, the remaining of the proof remains identical; one just needs to replace the occurrences of
1410 $\mathbb{E}_{s \sim \xi_{\pi_b}} |V^{\bar{\pi}}(s) - \bar{V}^{\bar{\pi}}(\phi(s))|$ by $\mathbb{E}_{s \sim \xi_{\pi_b}} |U^{\bar{\pi}}(s) - \bar{U}^{\bar{\pi}}(\phi(s))|$.
1411

1412 Since the subsequent results all rely on Lemma 4 and Theorem 2, they all extend to episodic value functions.
1413

1414 **Theorem 3.** (Deep, Safe Policy Improvement) *Under the same preamble as in Thm. 2, assume that ϕ is fixed during
1415 the policy update and the behavioral is a latent policy with $\pi_b := \bar{\pi}_b \circ \phi$ and $\bar{\pi}_b \in \bar{\Pi}$. Then, the improvement of the
1416 return of \mathcal{M} under $\bar{\pi}$ can be guaranteed on π_b as*

$$1417 \quad \rho(\bar{\pi} \circ \phi, \mathcal{M}) - \rho(\pi_b, \mathcal{M}) \geq \rho(\bar{\pi}, \bar{\mathcal{M}}) - \rho(\bar{\pi}_b, \bar{\mathcal{M}}) - \zeta,$$

$$1418 \quad \text{where } \zeta := \text{AEL}(\pi_b) \cdot \left(\frac{L_R^{\xi_{\pi_b}}}{\gamma} + K_V L_P^{\xi_{\pi_b}} \right) \left(\frac{1}{1/D_{\text{IR}}^{\text{sup}}(\pi_b, \bar{\pi})} + \frac{1}{1-\gamma} \right).$$

1420 *Proof.* First, note that
1421

$$1422 \quad \rho(\bar{\pi} \circ \phi, \mathcal{M}) - \rho(\pi_b, \mathcal{M})$$

$$1423 \quad = \rho(\bar{\pi} \circ \phi, \mathcal{M}) - \rho(\bar{\pi}, \bar{\mathcal{M}}) + \rho(\bar{\pi}, \bar{\mathcal{M}}) - \rho(\pi_b, \mathcal{M}). \quad (14)$$

1424 By Theorem 2, we have with $D_{\text{IR}}^{\text{sup}}(\pi_b, \pi_b) = 1$ that

$$1426 \quad |\rho(\pi_b, \mathcal{M}) - \rho(\bar{\pi}_b, \bar{\mathcal{M}})| \leq \mathbb{E}_{\pi_b}^{\mathcal{M}} [\mathbf{T}] \cdot \frac{L_R^{\xi_{\pi_b}}/\gamma + K_V \cdot L_P^{\xi_{\pi_b}}}{1-\gamma},$$

1428 which implies that

$$1430 \quad \rho(\pi_b, \mathcal{M}) - \rho(\bar{\pi}_b, \bar{\mathcal{M}}) \leq \mathbb{E}_{\pi_b}^{\mathcal{M}} [\mathbf{T}] \cdot \frac{L_R^{\xi_{\pi_b}}/\gamma + K_V \cdot L_P^{\xi_{\pi_b}}}{1-\gamma}$$

$$1433 \quad \iff \rho(\pi_b, \mathcal{M}) \leq \rho(\bar{\pi}_b, \bar{\mathcal{M}}) + \mathbb{E}_{\pi_b}^{\mathcal{M}} [\mathbf{T}] \cdot \frac{L_R^{\xi_{\pi_b}}/\gamma + K_V \cdot L_P^{\xi_{\pi_b}}}{1-\gamma}. \quad (15)$$

1435 On the other hand, we have
1436

$$1437 \quad |\rho(\bar{\pi} \circ \phi, \mathcal{M}) - \rho(\bar{\pi}, \bar{\mathcal{M}})| \leq \mathbb{E}_{\pi_b}^{\mathcal{M}} [\mathbf{T}] \cdot \frac{L_R^{\xi_{\pi_b}}/\gamma + K_V \cdot L_P^{\xi_{\pi_b}}}{1/D_{\text{IR}}^{\text{sup}}(\pi_b, \bar{\pi}) - \gamma},$$

1439 which implies that
1440

$$1441 \quad \rho(\bar{\pi} \circ \phi, \mathcal{M}) - \rho(\bar{\pi}, \bar{\mathcal{M}}) \geq -\mathbb{E}_{\pi_b}^{\mathcal{M}} [\mathbf{T}] \cdot \frac{L_R^{\xi_{\pi_b}}/\gamma + K_V \cdot L_P^{\xi_{\pi_b}}}{1/D_{\text{IR}}^{\text{sup}}(\pi_b, \bar{\pi}) - \gamma}. \quad (16)$$

1443 By plugging Equations 15 and 16 into Equation 14, we get the desired result:
1444

$$1445 \quad \rho(\bar{\pi} \circ \phi, \mathcal{M}) - \rho(\pi_b, \mathcal{M})$$

$$1446 \quad = \underbrace{\rho(\bar{\pi} \circ \phi, \mathcal{M}) - \rho(\bar{\pi}, \bar{\mathcal{M}})}_{\geq} + \rho(\bar{\pi}, \bar{\mathcal{M}}) - \underbrace{\rho(\pi_b, \mathcal{M})}_{\leq}$$

$$1447 \quad - \mathbb{E}_{\pi_b}^{\mathcal{M}} [\mathbf{T}] \cdot \frac{L_R^{\xi_{\pi_b}}/\gamma + K_V \cdot L_P^{\xi_{\pi_b}}}{1/D_{\text{IR}}^{\text{sup}}(\pi_b, \bar{\pi}) - \gamma} \quad \rho(\bar{\pi}_b, \bar{\mathcal{M}}) + \mathbb{E}_{\pi_b}^{\mathcal{M}} [\mathbf{T}] \cdot \frac{L_R^{\xi_{\pi_b}}/\gamma + K_V \cdot L_P^{\xi_{\pi_b}}}{1-\gamma}$$

$$1453 \quad \geq -\mathbb{E}_{\pi_b}^{\mathcal{M}} [\mathbf{T}] \cdot \frac{L_R^{\xi_{\pi_b}}/\gamma + K_V \cdot L_P^{\xi_{\pi_b}}}{1/D_{\text{IR}}^{\text{sup}}(\pi_b, \bar{\pi}) - \gamma} + \rho(\bar{\pi}, \bar{\mathcal{M}}) - \rho(\bar{\pi}_b, \bar{\mathcal{M}}) - \mathbb{E}_{\pi_b}^{\mathcal{M}} [\mathbf{T}] \cdot \frac{L_R^{\xi_{\pi_b}}/\gamma + K_V \cdot L_P^{\xi_{\pi_b}}}{1-\gamma}$$

$$1456 \quad = \rho(\bar{\pi}, \bar{\mathcal{M}}) - \rho(\bar{\pi}_b, \bar{\mathcal{M}}) - \mathbb{E}_{\pi_b}^{\mathcal{M}} [\mathbf{T}] \left(\frac{L_R^{\xi_{\pi_b}}/\gamma + K_V \cdot L_P^{\xi_{\pi_b}}}{1/D_{\text{IR}}^{\text{sup}}(\pi_b, \bar{\pi}) - \gamma} + \frac{1}{1-\gamma} \right).$$

□

1458 In the following, we provide a probabilistic version of Theorem 3, as it is standard in the SPI literature. Essentially,
 1459 we derive probably approximately correct estimations from interaction data of L_R, L_P . Then, we use those
 1460 estimations to get an approximation of ζ , the error term of the safe policy improvement inequality of Theorem 3.

1461 Those PAC guarantees rely on a discrete latent space. While it may seem restrictive, learning discrete latent spaces
 1462 turns out to be beneficial not only theoretically (e.g., it yields trivial Lipschitz bounds on the latent reward and
 1463 transition functions), but also in practice (see, e.g., Hafner et al., 2021).

1464 Finally, note that we provide two versions of the theorem: (1) one where we have access to an upper bound of the
 1465 AEL (which is mild in practice), and (2) another one where this bound cannot be derived. The latter case yields
 1466 an additional challenge as we need to estimate the AEL from sample states drawn according to the stationary
 1467 distribution. In this case, the bound yields a probabilistic algorithm that is guaranteed to almost surely terminate
 1468 without any predefined endpoint, as it depends on the current approximation of the losses.

1469 **Theorem 5** (Probabilistic Deep SPI with confidence bound). *Under the same preamble as in Theorem 3, assume
 1470 now \mathcal{S} is discrete. Let $\{\langle s_t, a_t, r_t, s'_t \rangle : 1 \leq t \leq T\}$ be a set of T transitions drawn from ξ_{π_b} by simulating \mathcal{M}_{π_b} ,
 1471 i.e., $s_t \sim \xi_{\pi_b}$, $a_t \sim \pi_b(\cdot | s_t)$, $r_t = R(s_t, a_t)$, and $s'_t \sim P(\cdot | s_t, a_t)$ for all $1 \leq t \leq T$. Let $\varepsilon, \delta > 0$ and define*

$$1474 \quad \hat{L}_P := 1 - \frac{1}{T} \sum_{t=1}^T \bar{P}(\phi(s'_t) | \phi(s_t), a_t), \quad \hat{L}_R := \frac{1}{T} \sum_{t=1}^T |r_t - \bar{R}(\phi(s_t), a_t)|, \quad \hat{\xi}_{\text{reset}} := \frac{1}{T} \sum_{t=0}^T \mathbb{1}_{\{s_t = s_{\text{reset}}\}},$$

1477 $\kappa := \frac{1}{1/D_{IR}^{\text{sup}}(\pi_b, \bar{\pi}) - \gamma} + \frac{1}{1 - \gamma}$, and $R^* := \max\{1, 4R_{\text{MAX}}^2\}$. Then, the policy can be safely improved as
 1478

$$1479 \quad \rho(\bar{\pi} \circ \phi, \mathcal{M}) - \rho(\pi_b, \mathcal{M}) \geq \rho(\bar{\pi}, \bar{\mathcal{M}}) - \rho(\bar{\pi}_b, \bar{\mathcal{M}}) - \hat{\zeta}, \quad (17)$$

1480 with probability at least $1 - \delta$ under the following conditions:

1481 (1) one has access to an upper bound $L \geq \text{AEL}(\pi_b)$, the number of collected transitions is lower-bounded by
 1482 $T \geq L^2 \cdot \left\lceil \frac{-R^* \log(\frac{\delta}{2} \cdot \kappa^2 (1/\gamma + K_V)^2)}{\varepsilon^2} \right\rceil$, and $\hat{\zeta} := L \cdot (\hat{L}_R/\gamma + K_V \hat{L}_P) \kappa + \varepsilon$; or

1485 (2) without access to such a bound, we take

$$1486 \quad T \geq \left\lceil \frac{-R^* \log(\delta/3)}{2} \cdot \max \left\{ \frac{1}{\hat{\xi}_{\text{reset}}^2}, \left(\frac{\kappa / \hat{\xi}_{\text{reset}} (\hat{L}_R/\gamma + K_V \hat{L}_P) + \varepsilon + \kappa \cdot (1/\gamma + K_V)}{\varepsilon \hat{\xi}_{\text{reset}}} \right)^2 \right\} \right\rceil,$$

$$1490 \quad \text{and } \hat{\zeta} := \frac{1}{\hat{\xi}_{\text{reset}}} (\hat{L}_R/\gamma + K_V \hat{L}_P) \kappa + \varepsilon.$$

1493 *Proof.* Let $\varepsilon, \delta > 0$. First, note that we need $T \geq \left\lceil \frac{-R^* \log(\delta/2)}{\varepsilon^2} \right\rceil$, to satisfy both (a) $\hat{L}_R + \varepsilon > L_R^{\xi_{\pi_b}}$ and
 1494 (b) $\hat{L}_P + \varepsilon > L_P^{\xi_{\pi_b}}$ with probability $1 - \delta$ and $T \geq \left\lceil \frac{-R^* \log(\delta/3)}{\varepsilon^2} \right\rceil$ to satisfy simultaneously (a), (b), and (c)
 1495 $\hat{\xi}_{\text{reset}} - \varepsilon < \xi_{\pi_b}(s_{\text{reset}})$ with probability $1 - \delta$. This statement is proven by Delgrange et al. (2022) and Delgrange
 1496 et al. (2025). The result is essentially due to a raw application of Hoeffding's inequality and the fact that Wasserstein
 1497 boils down to total variation when the state space is discrete (Villani, 2009).

1499 Let $\varepsilon' > 0$.

1500 **Case 1.** Assume we have an upper bound on $\text{AEL}(\pi_b)$, say L . Then it follows that

$$1503 \quad \zeta \leq L \cdot \left(\frac{L_R^{\xi_{\pi_b}}}{\gamma} + K_V L_P^{\xi_{\pi_b}} \right) \cdot \kappa \quad (\zeta \text{ is the safe policy improvement error term of Theorem 3})$$

$$1504$$

$$1505 \quad \leq L \cdot \left(\frac{\hat{L}_R + \varepsilon'}{\gamma} + K_V (\hat{L}_P + \varepsilon') \right) \cdot \kappa,$$

1507 with probability at least $1 - \delta$ whenever

$$1508 \quad T \geq \frac{-R^* \log(\delta/2)}{\varepsilon'^2}.$$

1510 To ensure an error of at most ε , choose ε' such that

$$1511 \quad L \cdot \left(\frac{\hat{L}_R + \varepsilon'}{\gamma} + K_V (\hat{L}_P + \varepsilon') \right) \kappa \leq L \cdot \left(\frac{\hat{L}_R}{\gamma} + K_V \hat{L}_P \right) \kappa + \varepsilon.$$

1512 Equivalently,

$$1514 \quad L\kappa\left(\frac{\varepsilon'}{\gamma} + K_V\varepsilon'\right) \leq \varepsilon \\ 1515 \quad \Leftrightarrow \varepsilon' \leq \frac{\varepsilon}{L\kappa(1/\gamma + K_V)}.$$

1517 Thus, it suffices that

$$1519 \quad T \geq \frac{-R^* \log(\delta/2)}{\varepsilon'^2} \geq \frac{-R^* \log(\delta/2)}{\varepsilon^2} (L\kappa(1/\gamma + K_V))^2$$

1521 to satisfy $\zeta \leq \hat{\zeta}$ with probability at least $1 - \delta$.

1522 **Case 2.** Suppose we do not have an upper bound on $\text{AEL}(\pi_b)$. From the proof of Theorem 2, we know that
1523 $\text{AEL}(\pi_b) = 1/\xi_{\pi_b}(s_{\text{reset}})$. In this case we include an estimate $\hat{\xi}_{\text{reset}}$ in the bound and use the high-probability
1524 deviations

$$1525 \quad \hat{L}_R + \varepsilon' > L_R^{\xi_{\pi_b}}, \quad \hat{L}_P + \varepsilon' > \hat{L}_P, \quad \hat{\xi}_{\text{reset}} - \varepsilon' < \xi_{\pi_b}(s_{\text{reset}}).$$

1527 We have

$$1528 \quad \zeta = \frac{1}{\xi_{\pi_b}(s_{\text{reset}})} \left(\frac{L_R}{\gamma} + K_V L_P \right) \kappa \quad (18)$$

$$1530 \quad \leq \frac{1}{\hat{\xi}_{\text{reset}} - \varepsilon'} \left(\frac{\hat{L}_R + \varepsilon'}{\gamma} + K_V(\hat{L}_P + \varepsilon') \right) \kappa, \quad (19)$$

1533 with probability at least $1 - \delta$ whenever

$$1534 \quad T \geq \frac{R^* \log(\delta/3)}{2\varepsilon'^2}.$$

1536 To guarantee an error at most ε , we require

$$1537 \quad \frac{1}{\hat{\xi}_{\text{reset}}} \left(\frac{\hat{L}_R}{\gamma} + K_V \hat{L}_P \right) \kappa + \varepsilon \geq \frac{1}{\hat{\xi}_{\text{reset}} - \varepsilon'} \left(\frac{\hat{L}_R + \varepsilon'}{\gamma} + K_V(\hat{L}_P + \varepsilon') \right) \kappa. \quad (20)$$

1540 Assuming $\varepsilon' < \hat{\xi}_{\text{reset}}$, we multiply both sides of (20) by $(\hat{\xi}_{\text{reset}} - \varepsilon')$ and expand:

$$1541 \quad \left(\frac{\hat{L}_R}{\gamma} + K_V \hat{L}_P \right) \kappa \left(1 - \frac{\varepsilon'}{\hat{\xi}_{\text{reset}}} \right) + \varepsilon \hat{\xi}_{\text{reset}} - \varepsilon \varepsilon' \\ 1542 \quad \geq \left(\frac{\hat{L}_R}{\gamma} + K_V \hat{L}_P \right) \kappa + \left(\frac{1}{\gamma} + K_V \right) \kappa \varepsilon'.$$

1545 Cancel the common term $(\frac{\hat{L}_R}{\gamma} + K_V \hat{L}_P) \kappa$ and group the ε' terms:

$$1547 \quad \varepsilon \hat{\xi}_{\text{reset}} \geq \varepsilon' \left[\frac{\kappa}{\hat{\xi}_{\text{reset}}} \left(\frac{\hat{L}_R}{\gamma} + K_V \hat{L}_P \right) + \varepsilon + \left(\frac{1}{\gamma} + K_V \right) \kappa \right].$$

1549 Therefore a sufficient condition is the explicit upper bound

$$1551 \quad \varepsilon' < \min \left\{ \hat{\xi}_{\text{reset}}, \frac{\varepsilon \hat{\xi}_{\text{reset}}}{\frac{\kappa}{\hat{\xi}_{\text{reset}}} \left(\frac{\hat{L}_R}{\gamma} + K_V \hat{L}_P \right) + \varepsilon + \left(\frac{1}{\gamma} + K_V \right) \kappa} \right\}. \quad (21)$$

1555 Together with the concentration requirement on T , the choice (21) ensures an error on ζ of at most ε with probability
1556 at least $1 - \delta$.

1557 Finally, the safe policy improvement bound follows from the fact that $\hat{\zeta}$ is greater than ζ with probability $1 - \delta$.
1558 Then, due to the SPI bound of Theorem 3, the improvement is guaranteed to be even larger when using ζ instead of
1559 $\hat{\zeta}$ as error term. This guarantees the improvement when $\hat{\zeta}$ is small enough. \square

1561 *Remark 3* (Episodic assumption). For the sake of presentation, we have considered and proved the bounds for
1562 episodic processes (cf. Appendix A). One could extend them to more general cases under the assumption that
1563 one has access to a stationary distribution ξ_{π_b} of \mathcal{M} . As mentioned in Section 2, the existence of a stationary
1564 distribution is often assumed in continual RL (Sutton and Barto, 2018) and guaranteed unique in the episodic case
1565 (Huang, 2020). Then, replacing the difference of returns in Theorem 3 by an expectation (similar to Theorem 2 with
1566 Lemma 4) would allow to remove the AEL term and obtain similar results.

1566

1567

1568 **Theorem 4.** (Deep SPI for representation learning) *Under the same preamble as in Thm. 2, let $\varepsilon > 0$ and*
 1569 $\delta := 4 \cdot \frac{L_R^{\xi_{\pi_b}} + \gamma K_V \cdot L_P^{\xi_{\pi_b}}}{\varepsilon \cdot (1/D_{\text{IR}}^{\sup}(\pi_b, \bar{\pi}) - \gamma)}$. *Then, with probability at least $1 - \delta$ under ξ_{π_b} , we have for all $s_1, s_2 \in \mathcal{S}$ that*

1571

1572

$$1573 \quad |V^{\bar{\pi}}(s_1) - V^{\bar{\pi}}(s_2)| \leq K_V \cdot \bar{d}(\phi(s_1), \phi(s_2)) + \varepsilon.$$

1574

1575

1576

1577

1578 *Proof.* First, let us consider bounding the following absolute value difference for every possible state $s \in \mathcal{S}$, i.e.,
 1579 $|V^{\bar{\pi}}(s) - \bar{V}^{\bar{\pi}}(\phi(s))|$. To that aim, we consider Markov's inequality:⁴

1580

1581

1582

1583

1584

1585

1586

1587

1588

1589

1590

1591 Consider any joint distribution $\lambda \in \Lambda(\xi_{\pi_b}, \xi_{\pi_b})$, i.e., any joint distribution over $\mathcal{S} \times \mathcal{S}$ whose marginals both match
 1592 ξ_{π_b} . Then, by the union bound, we have

1593

1594

1595

1596

1597

1598

1599

1600

1601

1602

1603

1604

1605

1606

1607

1608

1609

1610

1611

1612

1613

1614

1615

1616

1617

1618

1619

$$\begin{aligned} & \xi_{\pi_b}(\{s \in \mathcal{S}: |V^{\bar{\pi}}(s) - \bar{V}^{\bar{\pi}}(\phi(s))| > \varepsilon/2\}) \\ & \leq \xi_{\pi_b}(\{s \in \mathcal{S}: |V^{\bar{\pi}}(s) - \bar{V}^{\bar{\pi}}(\phi(s))| \geq \varepsilon/2\}) \\ & \leq 2 \cdot \frac{\mathbb{E}_{s \sim \xi_{\pi_b}} |V^{\bar{\pi}}(s) - \bar{V}^{\bar{\pi}}(\phi(s))|}{\varepsilon} && \text{(Markov's inequality)} \\ & \leq 2 \cdot \frac{L_R^{\xi_{\pi_b}} + \gamma K_V \cdot L_P^{\xi_{\pi_b}}}{\varepsilon \cdot (1/D_{\text{IR}}^{\sup}(\pi_b, \bar{\pi}) - \gamma)}. && \text{(by Lemma 4)} \end{aligned}$$

1589

1590

1591 Consider any joint distribution $\lambda \in \Lambda(\xi_{\pi_b}, \xi_{\pi_b})$, i.e., any joint distribution over $\mathcal{S} \times \mathcal{S}$ whose marginals both match
 1592 ξ_{π_b} . Then, by the union bound, we have

1593

1594

1595

1596

1597

1598

1599

1600

1601

1602

1603

1604

1605

1606

1607

1608

1609

1610

1611

1612

1613

1614

1615

1616

1617

1618

1619

$$\begin{aligned} & \lambda(\{(s_1, s_2) \in \mathcal{S} \times \mathcal{S}: |V^{\bar{\pi}}(s_1) - \bar{V}^{\bar{\pi}}(\phi(s_1))| > \varepsilon/2 \text{ or } |V^{\bar{\pi}}(s_2) - \bar{V}^{\bar{\pi}}(\phi(s_2))| > \varepsilon/2\}) \\ & \leq \lambda(\{(s_1, s_2) \in \mathcal{S} \times \mathcal{S}: |V^{\bar{\pi}}(s_1) - \bar{V}^{\bar{\pi}}(\phi(s_1))| \geq \varepsilon/2 \text{ or } |V^{\bar{\pi}}(s_2) - \bar{V}^{\bar{\pi}}(\phi(s_2))| \geq \varepsilon/2\}) \\ & \leq \lambda(\{(s_1, s_2) \in \mathcal{S} \times \mathcal{S}: |V^{\bar{\pi}}(s_1) - \bar{V}^{\bar{\pi}}(\phi(s_1))| \geq \varepsilon/2\}) + \lambda(\{(s_1, s_2) \in \mathcal{S} \times \mathcal{S}: |V^{\bar{\pi}}(s_2) - \bar{V}^{\bar{\pi}}(\phi(s_2))| \geq \varepsilon/2\}) && \text{(union bound)} \\ & = \xi_{\pi_b}(\{s_1 \in \mathcal{S}: |V^{\bar{\pi}}(s_1) - \bar{V}^{\bar{\pi}}(\phi(s_1))| \geq \varepsilon/2\}) + \xi_{\pi_b}(\{s_2 \in \mathcal{S}: |V^{\bar{\pi}}(s_2) - \bar{V}^{\bar{\pi}}(\phi(s_2))| \geq \varepsilon/2\}) && \text{(\lambda has } \xi_{\pi_b} \text{ as marginal distributions)} \\ & \leq 4 \cdot \frac{L_R^{\xi_{\pi_b}} + \gamma K_V \cdot L_P^{\xi_{\pi_b}}}{\varepsilon \cdot (1/D_{\text{IR}}^{\sup}(\pi_b, \bar{\pi}) - \gamma)}. \end{aligned}$$

1604

1605

1606

1607

1608

1609

1610

1611

1612

1613

1614

1615

1616

1617

1618

1619

$$\begin{aligned} & |V^{\bar{\pi}}(s_1) - V^{\bar{\pi}}(s_2)| \\ & = |V^{\bar{\pi}}(s_1) - \bar{V}^{\bar{\pi}}(\phi(s_1)) + \bar{V}^{\bar{\pi}}(\phi(s_1)) - \bar{V}^{\bar{\pi}}(\phi(s_2)) + \bar{V}^{\bar{\pi}}(\phi(s_2)) - V^{\bar{\pi}}(s_2)| \\ & \leq |V^{\bar{\pi}}(s_1) - \bar{V}^{\bar{\pi}}(\phi(s_1))| + |\bar{V}^{\bar{\pi}}(\phi(s_1)) - \bar{V}^{\bar{\pi}}(\phi(s_2))| + |V^{\bar{\pi}}(s_2) - \bar{V}^{\bar{\pi}}(\phi(s_2))| && \text{(triangle inequality)} \\ & \leq |\bar{V}^{\bar{\pi}}(\phi(s_1)) - \bar{V}^{\bar{\pi}}(\phi(s_2))| + \varepsilon \\ & \leq K_V \cdot \bar{d}(\phi(s_1), \phi(s_2)) + \varepsilon. && \text{(by Lemma 3)} \end{aligned}$$

□

⁴also referred to as Chebyshev's inequality (Stein and Shakarchi, 2005).

1620 F DREAM SPI
16211622 **Algorithm 2:** DreamSPI

1624 **Input:** (others) world model and encoder parameters ϑ , actor/critic parameters ι , imagination
1625 horizon H
1626 Init. $s \in \mathcal{S}^{(T+1) \times B}$, $a \in \mathcal{A}^{T \times B}$, $r \in \mathbb{R}^{T \times B}$, $\bar{s} \in \bar{\mathcal{S}}^{(H+1) \times BT}$, $\bar{a} \in \mathcal{A}^{H \times BT}$, $\bar{r} \in \mathbb{R}^{H \times BT}$
1627 **repeat**
1628 **for** $t \leftarrow 1$ to T **do**
1629 $a_t \sim \bar{\pi}(\cdot | \phi(s_t))$
1630 $r_t, s_{t+1} \leftarrow \text{env.step}(s_t, a_t)$
1631 Update ϑ by descending $\nabla_\vartheta \text{DeepSPI_loss}(s, a, r, U^{\bar{\pi} \circ \phi}, \vartheta)$
1632 ▷ Only ϕ , \bar{P} , and \bar{R} are updated here
1633 world_model $\leftarrow \langle \bar{\mathcal{S}}, \mathcal{A}, \bar{P}, \bar{R} \rangle$
1634 Set latent start states: $\bar{s}_1 \leftarrow \{\phi(s_{t,i}) : 1 \leq t \leq T, 1 \leq i \leq B\}$
1635 Perform latent imagination:
1636 **for** $t \leftarrow 1$ to H **do**
1637 $\bar{a}_t \sim \bar{\pi}(\cdot | \bar{s}_t)$
1638 $\bar{r}_t, \bar{s}_{t+1} \leftarrow \text{world_model.step}(\bar{s}_t, \bar{a}_t)$
1639 Update ι by descending $\nabla_\iota \text{ppo_loss}(\bar{s}, \bar{a}, \bar{r}, A^{\bar{\pi}}, \iota)$
1640 ▷ Perform a standard PPO update of the actor/critic w.r.t. the imagined trajectories
1641 $s_1 \leftarrow s_{T+1}$
1642 **until** convergence
1643 **return** θ

1644 We report in Algorithm 2 the algorithm we used in our experiments to evaluate the quality of the world model’s
1645 predictions. Note that the algorithm is on-policy; we leverage parallelized environments to make sure data coming
1646 from the interaction covers sufficiently the state space (Mayor et al., 2025). Empirically, we found most beneficial
1647 to use discrete latent spaces, and model the transition function with categorical distributions (32 classes of 32
1648 categories, as in Dreamer; Hafner et al., 2021). This observation agrees with the observation made by Hafner et al.
1649 (2021) on the benefits of categorical latent spaces in world models.

1650

1651 G ADDITIONAL DETAILS ON THE ILLUSTRATIVE EXAMPLE
1652

1653

1654

1655

1656

1657

1658

1659

1660

1661

1662

1663

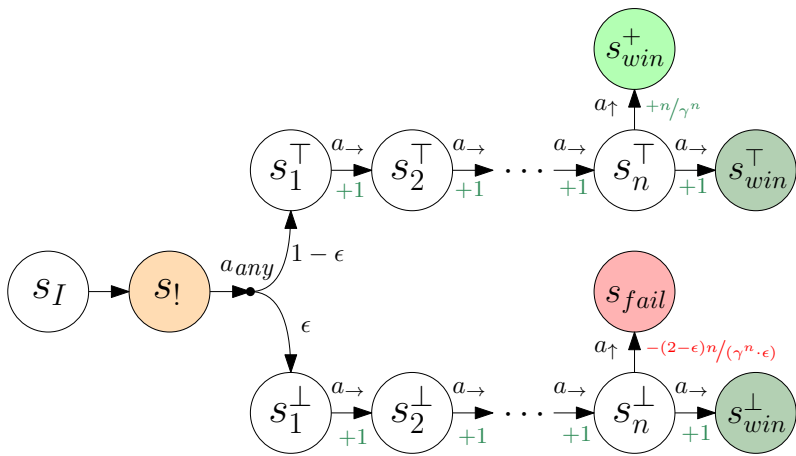
1664

1665

1666

1667

1668

1669 Figure 9: Underlying MDP of the grid world of Fig. 3. Actions leading to self-loops are omitted for clarity.
1670

1671 In this section, we expand on the illustrative example introduced in Sect. 6.1. The underlying MDP for the grid
1672 world is shown in Fig.9. Formally, the MDP has four actions a_{dir} with $\text{dir} \in \{\uparrow, \downarrow, \rightarrow, \leftarrow\}$, and $2n + 6$ states:

1673

- the initial state s_I , which transitions to $s_!$ whenever a_{\rightarrow} is played;

1674 • the hazardous state s_1 , sending the agent to s_1^\top with probability $1 - \epsilon$ and to s_1^\perp with probability ϵ , independently
 1675 of the action played;
 1676 • the $2n$ corridor states s_i^\top and s_i^\perp for $i \in \{1, \dots, n\}$, forming the top and bottom branches; and
 1677 • the terminal states s_{win}^\top , s_{win}^\perp , s_{fail}^\top , and s_{fail}^\perp .

1679 We focus on the value of the initial state $V^\pi(s_I)$ for policies $\pi \in \Pi$. We highlight three policies of particular
 1680 interest:

1681 (a) **The good** policy π_{good} : the policy moves right everywhere except in s_n^\top , where it chooses a_\uparrow :

$$\begin{aligned} 1683 \quad V^{\pi_{\text{good}}}(s_I) &= \gamma \left[(1 - \epsilon) \left(\sum_{t=1}^{n-1} \gamma^t + \gamma^n \cdot \frac{n}{\gamma^n} \right) + \epsilon \left(\sum_{t=1}^n \gamma^t \right) \right] \\ 1684 &= \gamma \left(\sum_{t=1}^{n-1} \gamma^t + (1 - \epsilon)n + \epsilon\gamma^n \right) \\ 1685 &= \gamma \left(\frac{\gamma - \gamma^n}{1 - \gamma} + (1 - \epsilon)n + \epsilon\gamma^n \right). \end{aligned}$$

1691 Learning π_{good} requires that the representation distinguishes the two branches and assigns distinct latent states
 1692 to s_n^\top and s_n^\perp . With $n = 5$, this corresponds to a return of ≈ 8.01 , which is the value reported in Fig. 4 for
 1693 DeepSPTI. This highlights the representation learning capabilities of our algorithm.

1694 (b) **The bad** policy π_{bad} : the policy moves right everywhere except in s_n^\top and s_n^\perp , where it chooses a_\uparrow :

$$\begin{aligned} 1695 \quad V^{\pi_{\text{bad}}}(s_I) &= \gamma \left[(1 - \epsilon) \left(\sum_{t=1}^{n-1} \gamma^t + \gamma^n \cdot \frac{n}{\gamma^n} \right) + \epsilon \left(\sum_{t=1}^{n-1} \gamma^t + \gamma^n \cdot \frac{-(2 - \epsilon)n}{\gamma^n \epsilon} \right) \right] \\ 1696 &= \gamma \left(\gamma \sum_{t=0}^{n-2} \gamma^t - n \right) \\ 1697 &= \gamma \left(\frac{\gamma - \gamma^n}{1 - \gamma} - n \right) \\ 1698 &< 0. \end{aligned}$$

1705 Such a policy may arise due to the policy confounding update described in Sect. 3.2, where the representation
 1706 incorrectly merges s_n^\top and s_n^\perp . With $n = 5$, this corresponds to a return of ≈ -1.09 .

1707 (c) ... and the ugly "always right" policy π_\rightarrow : this policy deterministically selects a_\rightarrow in every state. Its value is

$$1708 \quad V^{\pi_\rightarrow}(s_I) = \gamma \sum_{t=1}^n \gamma^t = \gamma^2 \sum_{t=0}^{n-1} \gamma^t = \frac{\gamma^2 - \gamma^{n+2}}{1 - \gamma}.$$

1711 With $n = 5$, this corresponds to a return of ≈ 4.8 . This coincides with the values reported in Fig. 4 for PPO,
 1712 indicating that PPO alone fails to address the confounding policy update in this example.

1713 As mentioned in the main text, we want to highlight the representation learning capabilities of DeepSPTI. For
 1714 this reason, we provide a view of the grid in raw pixels to the agent (cf. Fig. 10). In our experiments, we choose
 1715 $\epsilon = 0.2$. To evaluate PPO and DeepSPTI in this environment, we use the default parameters from cleanRL
 1716 (Huang et al., 2022), both for PPO and DeepSPTI. However, we enforce for both algorithms a compact, small
 1717 discrete representation with a limited capacity of 256 latent states (precisely, we use 4 categories of 4 classes,
 1718 with the same latent representation as the one used by Hafner et al., 2021). For DeepSPTI, we restrict the ratio to
 1719 $1/\gamma - 1$, which leads to a neighborhood constant $C < 1/\gamma$, as the theory suggests. Fig. 4 reports the median of 10
 1720 independent runs/seeds per algorithm, as well as the interquartile range (25-75%). Note that the values $V^\pi(s_I)$
 1721 reported in Fig. 4 are computed analytically.

1722

1723 H EXPERIMENTS: EVALUATION ON THE ATARI LEARNING ENVIRONMENTS

1724

1725 H.1 SETTING

1726

1727 Each presented experiment on the environments from ALE has been conducted across 8 seeds for each algorithm.
 1728 Each run requires (mean \pm std) 16.75 ± 1.7 min for PPO, 60.24 ± 20.16 min for DeepMDP, 62.49 ± 20.71 min for

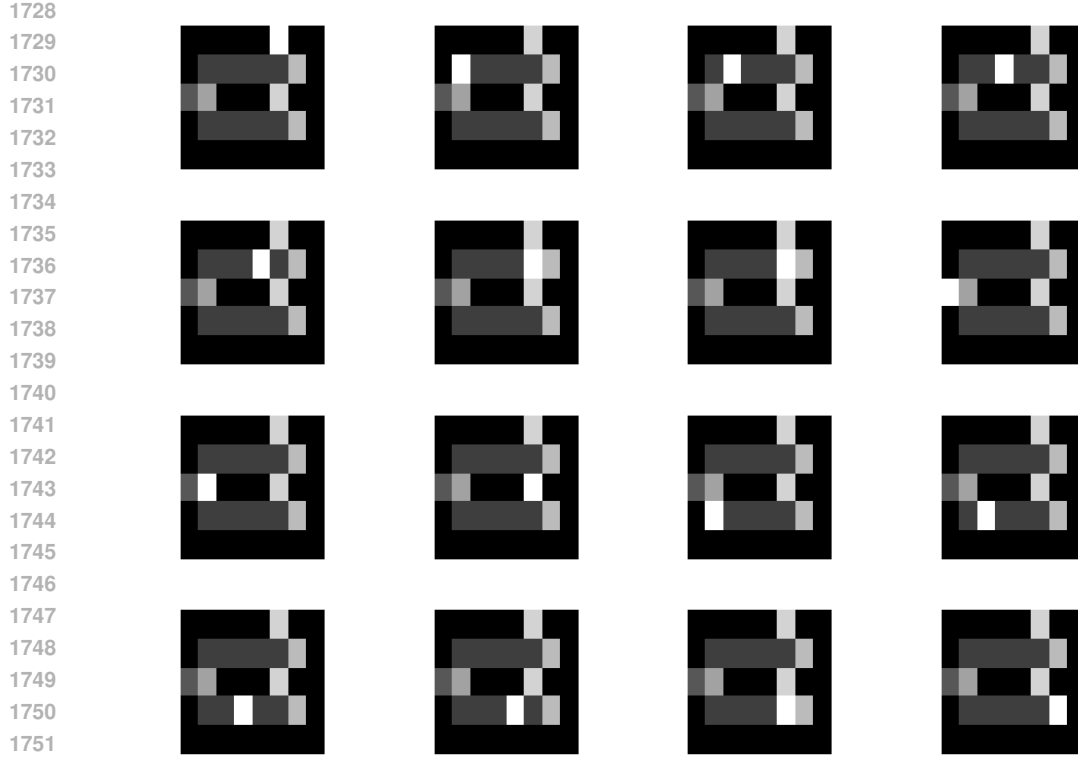


Figure 10: Observations of the grid perceived by the agent. The white-most cell corresponds to the agent’s location in the grid. Each observation has size 84×84 .

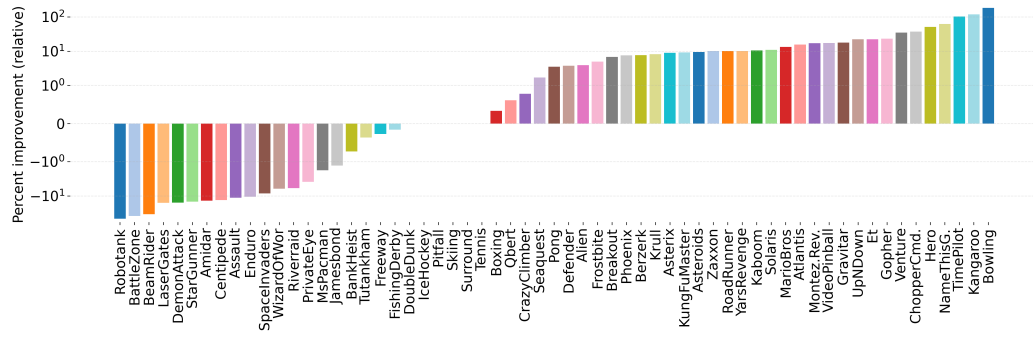


Figure 11: Relative improvement of DeepSPI compared to PPO over the full stochastic ALE suite (41/61).

DeepSPI, and 80.8 ± 1.35 min for DreamSPI on an NVIDIA A40. This corresponds to a $\approx 3.6 \times$ overhead when using DeepSPI instead of PPO, which we consider a modest cost given the guarantees we obtain. Because our method is on-policy and fully parallelizable, the wall-clock time remains well below that of off-policy approaches that do not exploit vectorized environments. For comparison, SAC requires roughly 40 hours for the same number of collected frames on an NVIDIA A100 (Huang et al., 2022), and Dreamer-v2 needs about two days on NVIDIA V100 (Hafner et al., 2021).

1777

1779 H.2 ADDITIONAL PLOTS

1780

1781 In this section, we present additional figures to highlight statistics and the performance of our algorithm, DeepSPI. Fig. 11 presents the relative improvement of DeepSPI w.r.t. PPO (Fig. 11). We formally compute the *relative*

1782 improvement as

$$\frac{\text{score} - \text{score}_{\text{baseline}}}{|\text{score}_{\text{baseline}}|}$$

1785 and we use the maximum median human normalized score as the metric to compare in each environment. See
 1786 next page for a comparison of each of the algorithms (average episodic return) per environment, across training
 1787 steps. We report the median and interquartile range (25–75%) for each environment. Recall that one training step
 1788 corresponds to gathering four Atari frames in the environment.

1789

1790 **Transition and reward losses.** In the main text, we stated that the transition loss achieved by DeepSPI is, in
 1791 general, lower than for DeepMDPs. We elaborate here on the statistical significance of this claim. First, as for the
 1792 human normalized score, we provide in Fig. 12 aggregate metrics for the transition and reward losses. This analysis
 1793 already reveals that there is no statistically significant difference between the capacity to predict rewards between
 1794 the two algorithms. We take a closer look at the transition loss.

1795 For each environment i , we summarize the transition loss of DeepSPI and DeepMDP by scalars ℓ_i^{SPI} and ℓ_i^{MDP} ,
 1796 and form paired differences $d_i = \ell_i^{\text{SPI}} - \ell_i^{\text{MDP}}$. The reported mean difference $\bar{d} = \frac{1}{n} \sum_i d_i = -0.1381$ therefore
 1797 means that, on average across environments, DeepSPI’s transition loss is about 0.14 units lower than DeepMDP’s.
 1798 To quantify uncertainty on this average effect, we use a paired bootstrap: we resample the n environments with
 1799 replacement, recompute $\bar{d}^{(b)}$ for each bootstrap sample $b = 1, \dots, B$, and form the 95% confidence interval as
 1800 the 2.5th and 97.5th percentiles of $\{\bar{d}^{(b)}\}_{b=1}^B$. The resulting interval $[-0.2226, -0.05907]$ lies entirely below zero,
 1801 which under the usual frequentist interpretation provides strong evidence that the true mean gap in transition loss is
 1802 negative (DeepSPI better) rather than a consequence of sampling noise.

1803 The paired Wilcoxon signed-rank test (Wilcoxon, 1992) further supports this conclusion without invoking normality
 1804 of the d_i : it ranks the absolute differences $|d_i|$, assigns each rank the sign of d_i , and uses the signed rank sum as a
 1805 test statistic for the null hypothesis $H_0 : \text{median}(d_i) = 0$. We obtain a very small two-sided p -value $p = 6.6 \times 10^{-4}$
 1806 indicating that observing differences this systematically negative would be extremely unlikely if DeepSPI and
 1807 DeepMDP had the same typical transition loss.

1808 Finally, the aggregates of Fig. 12 provide a complementary robust view: the interquartile mean (IQM) of transition
 1809 loss is lower for DeepSPI than for DeepMDP, indicating that DeepSPI improves not only the mean performance
 1810 but also the performance on the central bulk of environments. Taken together, the negative mean difference with
 1811 a 95% confidence interval that excludes zero, the significant Wilcoxon test, and the lower IQM all consistently
 1812 indicate that DeepSPI achieves statistically significantly lower transition loss than DeepMDP across Atari.

1813

1814 H.3 HYPERPARAMETERS

1815

1816 As mentioned in the main text, we use the same parameters for PPO as the default cleanRL’s parameters.
 1817 We list the DeepSPI parameters in Table 1 and those of DreamSPI in Table 2. We used the same pa-
 1818 rameters as DeepSPI for DeepMDPs. For DeepSPI, we performed a grid search for the transition density
 1819 in $\{\text{IndependentNormal}, \text{MixtureIndependentNormal}(n = 5), \text{Categorical}(n_{\text{cat}} = 32, n_{\text{cls}} = 32)\}$. The grid
 1820 search revealed that the mixture of independent normal distributions (i.e., with diagonal covariance matrices)
 1821 worked best for DeepSPI. We also found that using Lipschitz networks to enforce the Lipschitzness of the latent
 1822 space (cf. Sect. 5) was faster than enforcing a gradient penalty (as used by Gelada et al. 2019) since, in contrast to
 1823 gradient penalties, enforcing a Lipschitz condition through the architecture does not require additional sampling
 1824 from the latent transition function (which might turn out costly, especially with mixture distributions). Furthermore,
 1825 norm-constrained GroupSort architectures ensure Lipschitzness by construction. For the reward and transition
 1826 coefficients, we performed a grid search in $\alpha_R, \alpha_P \in \{10^{-2}, 5 \times 10^{-3}, 10^{-3}, 5 \times 10^{-4}, 10^{-4}\}$. We found the
 1827 best performance at $\alpha_R = 0.01$ and $\alpha_P = 5 \times 10^{-4}$.

1828

1829

1830

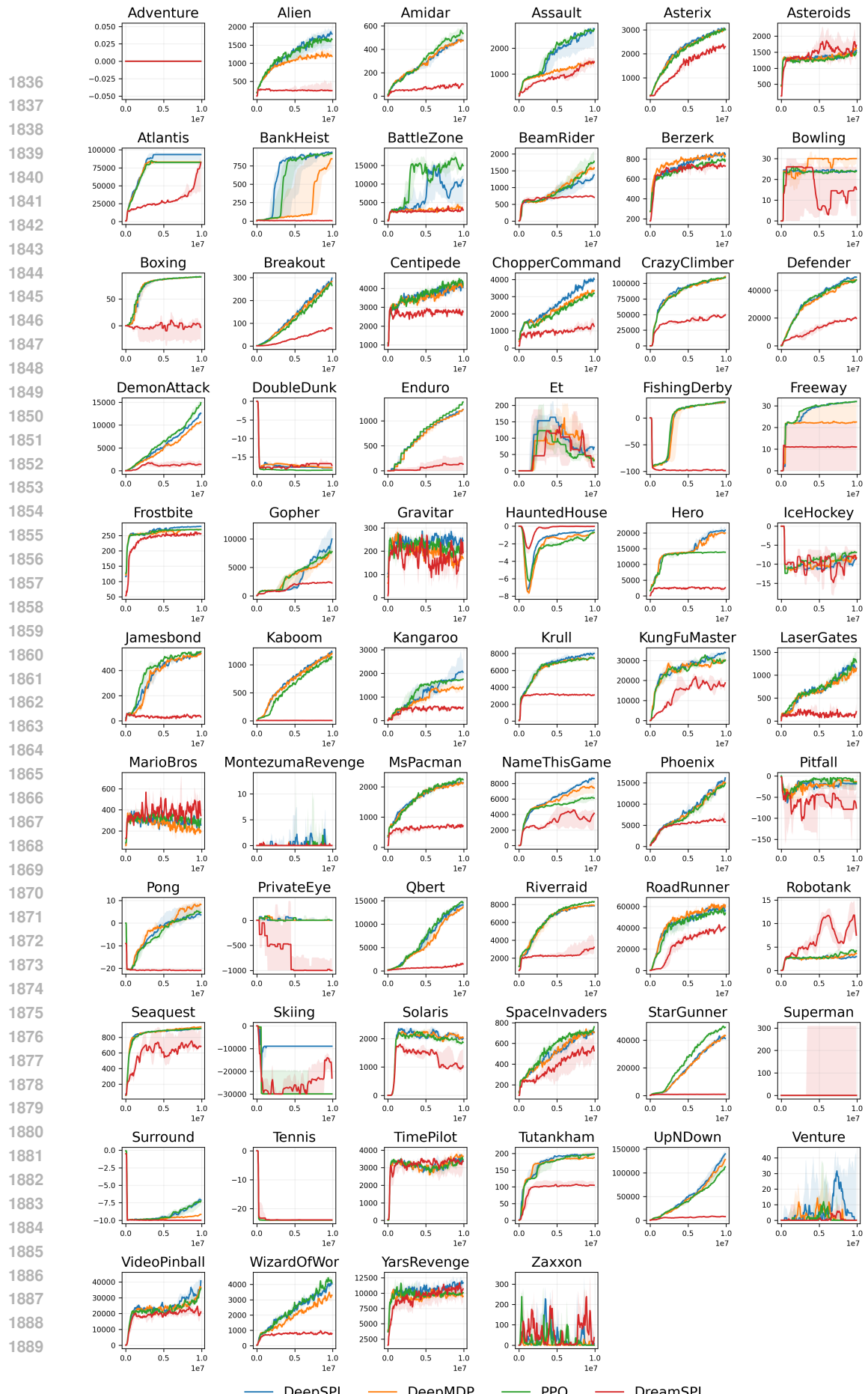
1831

1832

1833

1834

1835



1890

1891

1892

1893

1894

1895

1896

1897

1898

1899

1900

1901

1902

1903

1904

1905

1906

1907

1908

1909

1910

1911

1912

1913

1914

1915

1916

1917

1918

1919

1920

1921

1922

1923

1924

1925

1926

1927

1928

1929

1930

1931

1932

1933

1934

1935

1936

1937

1938

1939

1940

1941

1942

1943

Hyperparameter	Value
Learning rate	2.5×10^{-4}
Number of envs	128
Number of rollout steps	8
LR annealing	True
Activation function	ReLU
Discount factor γ	0.99
GAE λ	0.95
Number of minibatches	4
Update epochs	4
Advantage normalization	True
Clipping coefficient ϵ	0.1
Entropy coefficient	0.01
Value loss coefficient	0.5
Max gradient norm	0.5
Transition loss coefficient (α_P)	5×10^{-4}
Reward loss coefficient (α_R)	0.01
Transition density	Mixture of Normal (diagonal covariance matrix)
Number of distributions	5
Lipschitz networks	True

Table 1: Summary of DeepSPI hyperparameters.

Hyperparameter	Value
Imagination horizon	8
actor/critic update epochs	1
actor/critic number of minibatches	$4 \times 8 = 32$
Discount factor γ	0.995
Encoder learning rate	2×10^{-4}
Actor learning rate	2.75×10^{-5}
Critic learning rate	2.75×10^{-5}
World model learning rate	2×10^{-4}
Global LR annealing	False
Weight decay (AdamW)	True; with decay 10^{-6}
Transition density	Categorical (32 categories of 32 classes, see Hafner et al., 2021)
Transition loss coefficient (α_P)	0.01
Reward loss coefficient (α_R)	0.01
Lipschitz networks	False (unnecessary with discrete random variables)
Other parameters	Same as DeepSPI

Table 2: Summary of DreamSPI hyperparameters.

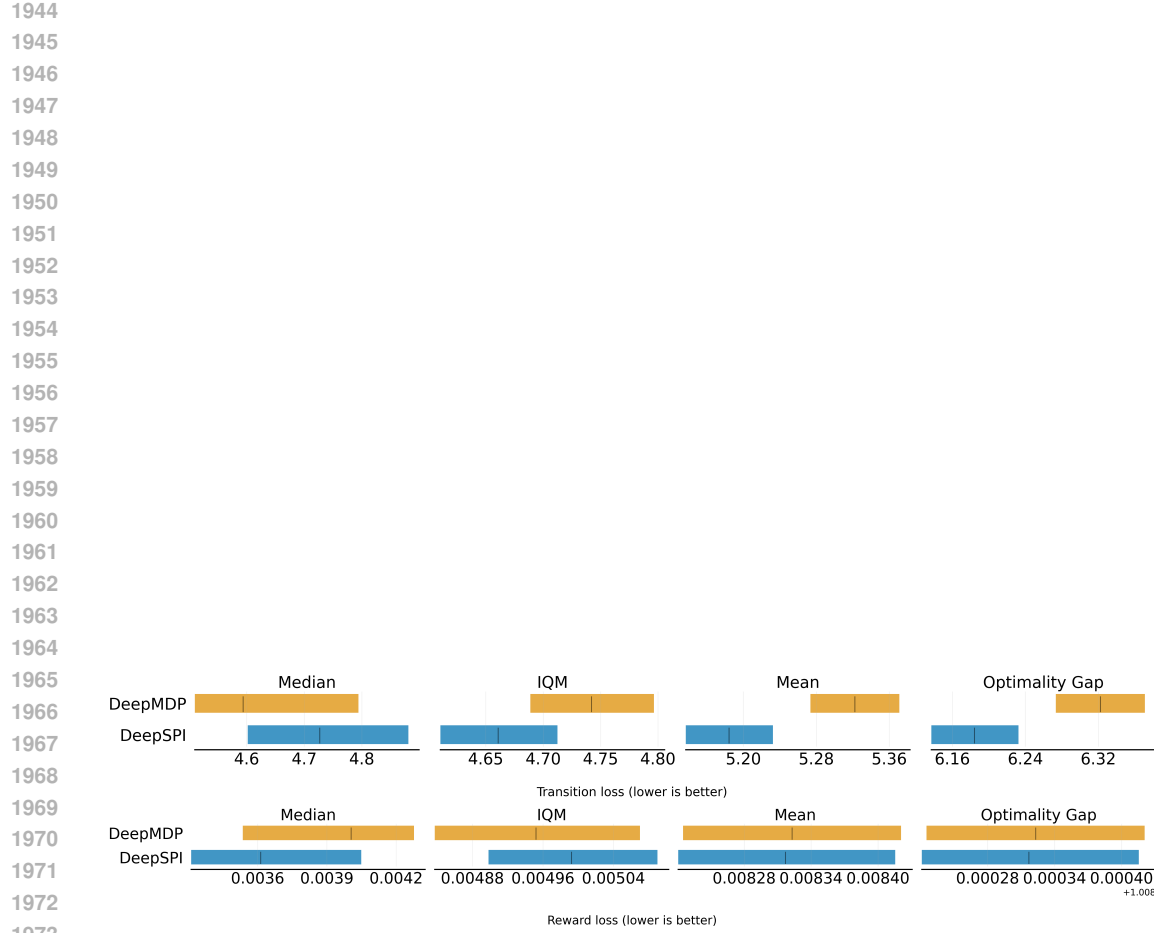


Figure 12: Aggregate median, IQR, Mean, and optimality gap for the reported transition and reward losses over all the Atari environments considered in our experiments, with 95% confidence intervals. The confidence intervals are obtained via percentile bootstrapping with stratified resampling. For more information, refer to Agarwal et al., 2021b.

1978
1979
1980
1981
1982
1983
1984
1985
1986
1987
1988
1989
1990
1991
1992
1993
1994
1995
1996
1997